FROM MUON TO GLUON: BRIDGING THEORY AND PRACTICE OF LMO-BASED OPTIMIZERS FOR LLMS

Anonymous authors
Paper under double-blind review

ABSTRACT

Recent developments in deep learning optimization have brought about radically new algorithms based on the Linear Minimization Oracle (LMO) framework, such as Muon (Jordan et al., 2024b) and Scion (Pethick et al., 2025b). After over a decade of Adam's dominance, these LMO-based methods are emerging as viable replacements, offering several practical advantages such as improved memory efficiency, better hyperparameter transferability, and most importantly, superior empirical performance on large-scale tasks, including LLM training. However, a significant gap remains between their practical use and our current theoretical understanding: prior analyses (1) overlook the layer-wise LMO application of these optimizers in practice, and (2) rely on an unrealistic smoothness assumption, leading to impractically small stepsizes. To address both, we propose a new LMO-based framework called Gluon, capturing prior theoretically analyzed methods as special cases, and introduce a new refined generalized smoothness model that captures the layer-wise geometry of neural networks, matches the layer-wise practical implementation of Muon and Scion, and leads to state-of-the-art convergence guarantees. Our experiments with `NanoGPT` and `CNN` confirm that our assumption holds along the optimization trajectory, ultimately closing the gap between theory and practice.

1 INTRODUCTION

The success of deep learning models across a wide range of challenging domains is inseparable from the optimization algorithms used to train them. As neural networks have grown deeper and datasets larger, optimization has quietly become one of the most consequential components of modern machine learning (ML). Nowhere is this more evident than in the training of large language models (LLMs), which routinely consume thousands of GPU-hours. Adam (Kingma & Ba, 2015) (and lately AdamW (Loshchilov & Hutter, 2019))—being effective, relatively reliable, and widely adopted—has for over a decade served as the default choice for this task. While this reliance has powered much of deep learning's progress, it has also exposed the shortcomings of adaptive moment estimation as a one-size-fits-all solution–namely, sensitivity to learning rate schedules, heavy tuning requirements (Wilson et al., 2017), and poor generalization when not carefully calibrated (Zou et al., 2021). However, a shift may now be underway. Recent optimizers, such as Muon (Jordan et al., 2024b) and Scion (Pethick et al., 2025b), represent a significant departure from Adam-type methods: they forgo the adaptive moment estimation in favor of a geometry-aware approach inspired by Frank-Wolfe algorithms (Frank & Wolfe, 1956; Pokutta, 2024). These optimizers are not only simpler to implement and easier to tune, but also appear empirically stronger, outperforming AdamW in LLM training (Liu et al., 2025; Pethick et al., 2025b).

Yet, despite their potential, these new methods are still in their infancy, and our understanding of their theoretical foundations and practical utility in LLM training remains incomplete. Prior convergence guarantees in realistic nonconvex regimes are still far from satisfactory. Indeed, as we argue in Section 2, the (very few) existing theoretical analyses *fail to capture the true algorithms used in practice*, focusing instead on simplified variants that diverge from actual implementations. We identify two key mismatches—*neglect of layer-wise structure* (Section 2.1) and flawed stepsize choices stemming from an *inaccurate smoothness model* (Section 2.2)—and close this gap with a *solution to both*. We elaborate on these advances in the remainder of the paper.

Algorithm 1 Gluon: Stochastic Adaptive Layer-Wise LMO-based Optimizer with Momentum

1: **Input:** Initial model parameters $X^0 = [X_1^0, \ldots, X_p^0] \in \mathcal{S}$, momentum $M^0 = [M_1^0, \ldots, M_p^0] \in \mathcal{S}$, momentum decay factors $\beta^k \in [0, 1)$ for all iterations $k \geq 0$
2: **for** $k = 0, 1, 2, \ldots, K-1$ **do**
3: Sample $\xi^k \sim \mathcal{D}$
4: **for** $i = 1, 2, \ldots, p$ **do**
5: Compute stochastic gradient $\nabla_i f_{\xi^k}(X^k)$ for layer i
6: Update momentum $M_i^k = \beta^k M_i^{k-1} + (1-\beta^k)\nabla_i f_{\xi^k}(X^k)$ for layer i
7: Choose adaptive stepsize/radius $t_i^k > 0$ for layer i
8: Update parameters for layer i via LMO over $\mathcal{B}_i^k := \{X_i \in \mathcal{S}_i : \|X_i - X_i^k\|_{(i)} \leq t_i^k\}$:

$$X_i^{k+1} = \mathrm{LMO}_{\mathcal{B}_i^k}\left(M_i^k\right) := \arg\min_{X_i \in \mathcal{B}_i^k} \langle M_i^k, X_i \rangle_{(i)} \tag{1}$$

9: **end for**
10: Update full parameter vector $X^{k+1} = [X_1^{k+1}, \ldots, X_p^{k+1}]$
11: **end for**

Our goal is to solve the general optimization problem

$$\min_{X \in \mathcal{S}} \left\{ f(X) := \mathbb{E}_{\xi \sim \mathcal{D}}\left[f_\xi(X)\right] \right\}, \tag{2}$$

where $\mathcal{S}$ is a finite-dimensional vector space and $f_\xi : \mathcal{S} \mapsto \mathbb{R}$ are potentially non-convex and non-smooth but continuously differentiable functions. Here, $f_\xi(X)$ represents the loss of model parameterized by X associated with training data point ξ sampled from probability distribution $\mathcal{D}$. To make the problem meaningful, we assume that $f^{\inf} := \inf_{X \in \mathcal{S}} f(X) > -\infty$. In this work we are particularly interested in the scenario when the parameter vector $X \in \mathcal{S}$ is obtained by collecting the matrices $X_i \in \mathcal{S}_i := \mathbb{R}^{m_i \times n_i}$ of trainable parameters across all layers $i = 1, \ldots, p$ of a deep model. For simplicity, we therefore write $X = [X_1, \ldots, X_p]$. This means that, formally, $\mathcal{S}$ is the d-dimensional product space $\mathcal{S} := \bigotimes_{i=1}^p \mathcal{S}_i \equiv \mathcal{S}_1 \otimes \cdots \otimes \mathcal{S}_p$, where $d := \sum_{i=1}^p m_i n_i$. With each space $\mathcal{S}_i$ we associate the trace inner product $\langle X_i, Y_i \rangle_{(i)} := \mathrm{tr}(X_i^\top Y_i)$ for $X_i, Y_i \in \mathcal{S}_i$, and an arbitrary norm $\|\cdot\|_{(i)}$, not necessarily induced by the inner product.

2 Theory vs. practice of Muon and Scion

In this work, we focus on an algorithm based on iteratively calling linear minimization oracles (LMOs) across all layers, formalized in Algorithm 1, for which we coin the name Gluon. In particular, for each layer i, independently across all layers, Gluon iteratively updates the parameters via

$$X_i^{k+1} = \mathrm{LMO}_{\mathcal{B}_i^k}(M_i^k) := \arg\min_{X_i \in \mathcal{B}_i^k} \langle M_i^k, X_i \rangle_{(i)}, \text{ where } \mathcal{B}_i^k := \{X_i \in \mathcal{S}_i : \|X_i - X_i^k\|_{(i)} \leq t_i^k\},$$

where $t_i^k > 0$ is an adaptively chosen stepsize/radius/learning rate.[1] Note that the momentum $M^k = [M_1^k, \ldots, M_p^k] \in \mathcal{S}$ accumulates the contributions from the stochastic gradients $\nabla f_{\xi^k}(X^k) = [\nabla_1 f_{\xi^k}(X^k), \ldots, \nabla_p f_{\xi^k}(X^k)] \in \mathcal{S}$ (see Step 6 of Algorithm 1).

The Gluon framework generalizes a range of methods, including Muon and Scion, which are recovered as special cases under specific norm choices (see Section 4.1 and Appendix D.1). Beyond their ability to outperform AdamW on large-scale benchmarks, these optimizers offer a number of attractive properties: improved memory efficiency, greater robustness to hyperparameter settings, and the ability to transfer those settings across model sizes (Pethick et al., 2025b; Shah et al., 2025). Moreover, in contrast to Adam, they were theoretically analyzed shortly after release and are guaranteed to converge under standard assumptions of Lipschitz smoothness[2] and bounded variance of stochastic gradients (Kovalev, 2025; Li & Hong, 2025; Pethick et al., 2025b).

[1] In this context, the radii defining the norm balls in the LMOs effectively act as stepsizes–see Appendix C.1. Accordingly, we use the terms *radius*, *stepsize*, and *learning rate* interchangeably throughout.

[2] A function $f : \mathcal{S} \mapsto \mathbb{R}$ is L-smooth if $\|\nabla f(x) - \nabla f(y)\|_\star \leq L \|x - y\|$ for all $x, y \in \mathcal{S}$, where $\mathcal{S}$ is a finite-dimensional vector space equipped with a norm $\|\cdot\|$ and $\|\cdot\|_\star$ is the dual norm associated with $\|\cdot\|$.

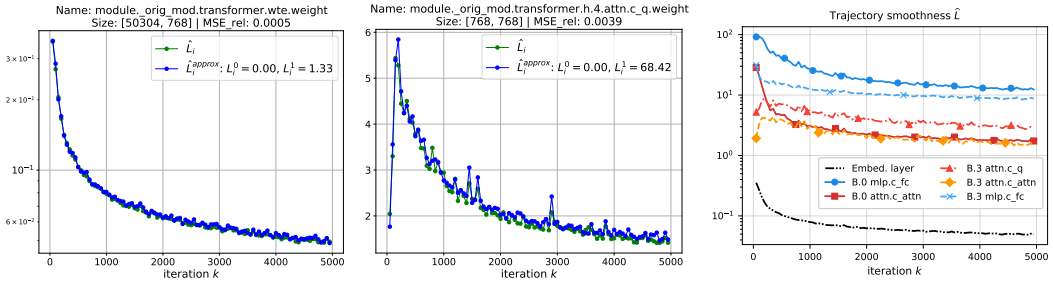

(a) Token embedding matrix from the first/last layer.

(b) Self-attention query matrix from the 4th transformer block.

(c) Trajectory smoothness across different blocks (B.i) and layers.

Figure 1: Training `NanoGPT` on `FineWeb` validates our layer-wise (L^0, L^1)-smoothness model.

Gluon presents the method that is deployed in practice (Jordan et al., 2024a; Pethick et al., 2025a) and has proven highly effective. That said, we argue that existing analyses (Kovalev, 2025; Li & Hong, 2025; Pethick et al., 2025b) do *not* accurately reflect this implementation, diverging from it in two key ways. As such, they *fail to explain why the algorithm performs so well*. Let us detail why.

2.1 Layer-wise structure

First, we briefly walk through the theoretical understanding offered by previous studies. Muon is an optimizer specifically designed for hidden layers, leaving the first and last layers to be handled by some other optimizer, e.g., Adam(W). Its original introduction by Jordan et al. (2024b) was purely empirical, with no attempt at theoretical analysis. The first convergence result came from Li & Hong (2025), who analyzed the smooth nonconvex setting but focused solely on problem (2) with $p = 1$, effectively limiting the scope to the single-layer case. The Scion[3] optimizer (a special case of Gluon) proposed by Pethick et al. (2025b) improves upon Muon by applying the LMO-based rule to all layers, ultimately achieving better empirical performance. Both this work and that of Kovalev (2025) analyze (a variant of) the general update rule

$$\begin{aligned} M^k &= \beta^k M^{k-1} + (1-\beta^k)\nabla f_{\xi^k}(X^k), \\ X^{k+1} &= \mathrm{LMO}_{\mathcal{B}^k}(M^k), \end{aligned} \tag{3}$$

where $\beta^k \in [0,1)$ is momentum, $\nabla f_{\xi^k}(X^k)$ is the stochastic gradient sampled at iteration k, and $\mathcal{B}^k := \{X \in \mathcal{S} : \|X - X^k\| \leq t^k\}$ is a norm ball centered at X^k with stepsize $t^k > 0$. This setup closely resembles the structure of Gluon, but is *not* exactly the same. Indeed, Gluon updates the parameters *layer-wise*, not jointly over the full vector X. This distinction is critical since for practical, extremely high-dimensional models, calculating a single global LMO for the entire parameter vector is prohibitively expensive, while breaking the problem into "smaller", per-layer LMOs restores computational feasibility.

Motivated by this disconnect, we formulate our analysis in the matrix product space $\mathcal{S}$, explicitly honoring the layer-wise structure. This enables us to study the actual per-layer updates (1), with assumptions and hyperparameters adapted to each layer.

2.2 A theory with predictive power

All prior works claiming to guarantee convergence of Algorithm 1 come with several serious analytical shortcomings–and these directly translate into practical deficiencies. Concretely, all existing analyses of Muon/Scion are built on the classical L-smoothness assumption, imposing a uniform smoothness constant across all layers. This is problematic, as *different layers have different geometries*, and thus *should be treated differently*.

But the issue runs much deeper. These algorithms are built for deep learning, where the objective functions are already well known *not* to be smooth (Crawshaw et al., 2022; Zhang et al., 2020). This mismatch has consequences: prior convergence analyses prescribe *tiny constant stepsizes* (see

[3] Pethick et al. (2025b) introduce two variants of the Scion optimizer: one for constrained optimization, called simply "Scion", and another for unconstrained problems, referred to as "unconstrained Scion". In this work, "Scion" refers to either variant, and "unScion" is used when referring to the unconstrained version.

Table 1), uniform across all parameter groups, which bear little resemblance to the tuned learning rates that yield state-of-the-art empirical performance in practice. Consequently, they completely fail to explain why these methods perform so well empirically. In other words, the theory falls short at the one thing it should do best: guiding practical choices, leaving practitioners reliant on costly manual tuning.

Our result in Theorem 1 shows this mismatch is *not* inevitable. To better reflect the behavior of deep models, we introduce a more expressive regularity condition: the *layer-wise* (L^0, L^1)*-smoothness*[4]–an extension of the generalized smoothness model of Zhang et al. (2020), applied at the layer level.

Assumption 1 (Layer-wise (L^0, L^1)-smoothness)**.** *The function $f : \mathcal{S} \mapsto \mathbb{R}$ is layer-wise (L^0, L^1)-smooth with constants $L^0 := (L_1^0, \ldots, L_p^0) \in \mathbb{R}_+^p$ and $L^1 := (L_1^1, \ldots, L_p^1) \in \mathbb{R}_+^p$. That is, the inequality*

$$\|\nabla_i f(X) - \nabla_i f(Y)\|_{(i)\star} \leq \left(L_i^0 + L_i^1 \|\nabla_i f(X)\|_{(i)\star}\right) \|X_i - Y_i\|_{(i)} \tag{4}$$

holds for all $i = 1, \ldots, p$ and all $X = [X_1, \ldots, X_p] \in \mathcal{S}$, $Y = [Y_1, \ldots, Y_p] \in \mathcal{S}$, where $\|\cdot\|_{(i)\star}$ is the dual norm associated with $\|\cdot\|_{(i)}$ (i.e., $\|X_i\|_{(i)\star} := \sup_{\|Z_i\|_{(i)} \leq 1} \langle X_i, Z_i \rangle_{(i)}$ for any $X_i \in \mathcal{S}_i$).

Assumption 1 can be viewed as a generalization of the anisotropic "vector" (L^0, L^1)–smoothness introduced by Liu et al. (2024) (now framed in terms of arbitrary norms), which itself is a generalization of the (L^0, L^1)–smoothness model of Zhang et al. (2020). As such, our analysis of Gluon goes beyond all existing results, which have only considered the classical L-smooth setting. Crucially, however, this is *not* generalization for its own sake–we argue that this is in fact *the right* model for the problem setting at hand. Why? There are (at least) two reasons.

First, unlike classical L-smoothness, our formulation *aligns very closely with empirical observations*. In Figures 1a and 1b, we validate Assumption 1 in the context of training `NanoGPT` on the `FineWeb` dataset. We plot estimated *trajectory smoothness* $\hat{L}_i[k]$ (defined in (10)) alongside the approximation $\hat{L}_i^{\text{approx}}[k] := L_i^0 + L_i^1 \|\nabla_i f_{\xi^{k+1}}(X^{k+1})\|_{(i)\star}$, where L_i^0, L_i^1 are layer-specific parameters estimated from the training run. The figures show these quantities for parameters from the embedding layer and one of the transformer blocks. The close correspondence between $\hat{L}_i[k]$ and $\hat{L}_i^{\text{approx}}[k]$ provides strong evidence that Assumption 1 holds approximately along the training trajectory. In Section 5, we further corroborate this finding, showing that our assumption is satisfied *across the entire model architecture* for both the `NanoGPT` language modeling task and a `CNN` trained on `CIFAR-10`. In all cases, we find that $L_i^0 \approx 0$ for all i, again highlighting the limitations of classical smoothness. Moreover, as shown in Figure 1c, trajectory smoothness varies substantially across blocks and layers, underscoring the need for per-layer treatment. Complementary experiments using AdamW as the optimizer (Figure 10) confirm that this heterogeneity is an intrinsic property of the loss landscape. Together, these results suggest that layer-wise (L^0, L^1)-smoothness offers a *significantly more realistic model of the loss landscape in modern deep learning*.

Secondly, Assumption 1 not only better captures the geometry of the models, but also *directly informs the design of adaptive and practically effective stepsizes*. In Theorem 1, we derive learning rates that reflect the local geometry of each parameter group, guided by our layer-wise smoothness model. As demonstrated in Section 5.1, our theoretically grounded stepsizes turn out to accurately capture the relative magnitudes of the layer-wise learning rates obtained by Pethick et al. (2025b) via hyperparameter tuning–a striking validation of our approach, which further highlights the need for layer-wise reasoning. This proves that *theoretical stepsizes can have predictive power* and effectively guide hyperparameter tuning.

3 Contributions

We present a comprehensive theoretical and empirical study of a broad class of layer-wise LMO-based optimization algorithms. Our key contributions can be summarized as follows:

[4]While we state Assumption 1 in this general form, it is worth noting that the proofs do not rely on its full strength. In all cases, we only require the assumption to hold for pairs X, Y such that $\|X - Y\| < c$ for some constant $c \geq 0$ (where $\|\cdot\|$ is any norm on $\mathcal{S}$). Specifically, the assumption is only invoked with $X = X^k$, $Y = X^{k+1}$, and since the stepsizes we use are bounded, the distances between consecutive iterates remain bounded as well. For clarity and consistency across results–since the relevant constants vary by theorem–we state the assumption in its stronger, global form, even though the local version suffices for all proofs.

Table 1: Comparison of convergence guarantees for Gluon (Algorithms 1 and 2) to achieve $\min_{k=0,\ldots,K-1} \sum_{i=1}^{p} \mathbb{E}[\|\nabla_i f(X^k)\|_{(i)\star}] \leq \varepsilon$, where the $\mathcal{O}(\cdot)$ notation hides logarithmic factors. Notation: K = total number of iterations, (L^0, L^1) = the result holds under layer-wise (L^0, L^1)-smoothness, t_i^k = radius/stepsize, $1-\beta^k$ = momentum.

Result	Stochastic?	(L^0, L^1)	Rate	Stepsizes t_i^k	$1-\beta^k$
(Kovalev, 2025, Theorem 1)	✗	✗	$\mathcal{O}\left(\frac{1}{K^{1/2}}\right)$	const $\propto \frac{1}{K^{1/2}}$ [b]	—
(Kovalev, 2025, Theorem 2)	✓	✗	$\mathcal{O}\left(\frac{1}{K^{1/4}}\right)$	const $\propto \frac{1}{K^{3/4}}$ [b]	const $\propto \frac{1}{K^{1/2}}$
(Li & Hong, 2025, Theorem 2.1)[a]	✓	✗	$\mathcal{O}\left(\frac{1}{K^{1/4}}\right)$	const $\propto \frac{1}{K^{3/4}}$ [b]	const $\propto \frac{1}{K^{1/2}}$
(Pethick et al., 2025b, Lemma 5.4)	✓	✗	$\mathcal{O}\left(\frac{1}{K^{1/4}}\right)$	const $\propto \frac{1}{K^{3/4}}$ [b]	$\propto \frac{1}{k^{1/2}}$
NEW: Theorem 1	✗	✓	$\mathcal{O}\left(\frac{1}{K^{1/2}}\right)$	Adaptive	—
NEW: Theorem 2	✓	✓	$\mathcal{O}\left(\frac{1}{K^{1/4}}\right)$	$\propto \frac{1}{k^{3/4}}$	$\propto \frac{1}{k^{1/2}}$

[a] Applies only to the Muon/Scion update in (13) with $p = 1$.
[b] These stepsizes are impractically tiny since they have an inverse dependence on the total number of iterations K.

◇ **A new generalized smoothness framework for neural networks.** We introduce *layer-wise* (L^0, L^1)*-smoothness* (Assumption 1), a novel non-Euclidean generalized smoothness condition that reflects the anisotropic, layer-wise structure of modern deep networks. This framework extends standard (L^0, L^1)-smoothness assumption (Zhang et al., 2020) to arbitrary norms while capturing per-layer variation, offering a *realistic foundation for analyzing deep learning optimizers*.

◇ **First principled analysis of layer-wise methods.** Building on our new assumption, we develop the first faithful convergence analysis for a class of LMO-based algorithms we term Gluon (Algorithms 1 and 2). We recover known algorithms, including state-of-the-art Muon-type optimizers, as special cases (Section 4.1 and Appendix D.1), and pinpoint why earlier theoretical works *fail* to explain the empirical success of these methods (Section 2). In contrast to prior analyses that oversimplify the update rules used in practice, our framework directly aligns with real-world implementations, bridging a critical gap between theory and application.

◇ **Sharper and more general convergence theory.** We develop a convergence theory that extends prior work in both scope and sharpness. In the deterministic case (Algorithm 2), we establish convergence for general non-convex objectives under our Assumption 1 (Theorem 1), and under the block-wise PŁ condition (Theorem 5). Unlike earlier analyses, our theory yields *adaptive, layer-wise stepsizes* that align remarkably well with those selected via tuning in large-scale experiments (Pethick et al., 2025b) (Section 5.1). We next analyze the practical stochastic variant with time-varying stepsizes and momentum (Algorithm 1), proving convergence under bounded variance assumption (Theorem 1). In both deterministic and stochastic regimes, our guarantees offer *tighter convergence rates* under *more general assumptions* (Table 1), providing the first such results the in non-smooth setting. Moreover, we provide the first theoretical explanation of the benefits of layer-wise learning rates, clearly establishing the advantages of structured, anisotropic optimization in deep learning.

◇ **Empirical evidence.** We validate our theoretical insights through extensive experiments (Section 5 and Appendix F) in both language modeling (`NanoGPT` on `FineWeb`) and image classification (`CNN` on `CIFAR-10`). The results confirm that our Assumption 1 holds approximately throughout training and demonstrate the practical utility of our theoretically prescribed stepsizes from Theorem 1.

4 Main Theory and Results

To gain a better intuition into the structure of the updates, we begin with a deterministic formulation of Gluon, formalized in Algorithm 2. At each iteration, the method independently minimizes a linear approximation of f around each parameter group X_i^k within a ball of radius $t_i^k > 0$, ultimately allowing for layer-specific algorithmic design choices.

4.1 Examples of optimizers satisfying our framework

Deterministic Gluon describes a general class of methods, parameterized by the choice of norms $\|\cdot\|_{(i)}$ in the LMO. To illustrate the flexibility of this framework, we highlight several notable special cases (see Appendix D.1 for more details). First, observe that the update rule (12) can be written as

$$X_i^{k+1} = X_i^k + t_i^k \mathrm{LMO}_{\{X_i \in \mathcal{S}_i : \|X_i\|_{(i)} \leq 1\}} \left(\nabla_i f(X^k)\right) = X_i^k + t_i^k \operatorname*{argmin}_{\|X_i\|_{(i)} \leq 1} \langle \nabla_i f(X^k), X_i \rangle_{(i)}. \quad (5)$$

For any $X_i \in \mathcal{S}_i = \mathbb{R}^{m_i \times n_i}$, define $\|X_i\|_{\alpha\to\beta} := \sup_{\|z\|_\alpha=1} \|X_i z\|_\beta$, where $\|\cdot\|_\alpha$ and $\|\cdot\|_\beta$ are some (possibly non-Euclidean) norms on $\mathbb{R}^{n_i}$ and $\mathbb{R}^{m_i}$, respectively. Note that (5) naturally recovers several known updates for specific choices of the layer norms, e.g., layer-wise normalized GD (Yu et al., 2018) for Euclidean norms $\|\cdot\|_{(i)} = \|\cdot\|_2$, and layer-wise signGD (Balles et al., 2020) for max-norms $\|\cdot\|_{(i)} = \|\cdot\|_\infty$. Two special cases are particularly relevant to our analysis:

$\diamond$ **Muon** (Jordan et al., 2024b) when $\|\cdot\|_{(i)} = \|\cdot\|_{2\to2}$ for all hidden layers.

$\diamond$ **unScion for LLM training** (Pethick et al., 2025b) when $\|\cdot\|_{(i)} = \sqrt{n_i/m_i}\|\cdot\|_{2\to2}$ for $i = 1,\dots,p-1$, corresponding to weight matrices of transformer blocks, and $\|\cdot\|_{(p)} = n_p\|\cdot\|_{1\to\infty}$ for the last group X_p, representing the embedding and output layers (the two coincide under the weight sharing regime[5] considered here). In this case, update (5) becomes

$$\begin{aligned} X_i^{k+1} &= X_i^k - t_i^k \sqrt{\frac{m_i}{n_i}} U_i^k \left(V_i^k\right)^\top, \quad i = 1,\dots,p-1, \\ X_p^{k+1} &= X_p^k - \frac{t_p^k}{n_p} \operatorname{sign}\left(\nabla_p f(X^k)\right), \end{aligned} \tag{6}$$

where the matrices U_i^k, V_i^k are obtained from the (reduced) SVD of $\nabla_i f(X^k) = U_i^k \Sigma_i^k \left(V_i^k\right)^\top$.

4.2 Convergence results

Having demonstrated the framework's flexibility through concrete examples, we now state a general convergence result for deterministic Gluon.

Theorem 1. *Let Assumption 1 hold and fix $\varepsilon > 0$. Let $X^0, \dots, X^{K-1}$ be the iterates of deterministic Gluon (Algorithm 2) run with stepsizes $t_i^k = \frac{\|\nabla_i f(X^k)\|_{(i)\star}}{L_i^0 + L_i^1 \|\nabla_i f(X^k)\|_{(i)\star}}$. Then, to guarantee that*

$$\min_{k=0,\dots,K-1} \sum_{i=1}^p \left[\frac{1/L_i^1}{\frac{1}{p}\sum_{j=1}^p 1/L_j^1} \left\|\nabla_i f(X^k)\right\|_{(i)\star} \right] \le \varepsilon, \tag{7}$$

it suffices to run the algorithm for

$$K = \left\lceil \frac{2\Delta^0 \left(\sum_{i=1}^p L_i^0/(L_i^1)^2\right)}{\varepsilon^2 \left(\frac{1}{p}\sum_{j=1}^p 1/L_j^1\right)^2} + \frac{2\Delta^0}{\varepsilon\left(\frac{1}{p}\sum_{j=1}^p 1/L_j^1\right)} \right\rceil \tag{8}$$

iterations, where $\Delta^0 := f(X^0) - f^{\inf}$.

Several important observations follow.

Convergence rate. In Appendix D.2, we prove an additional result (Theorem 3) that modifies the first term in (8) to $2\Delta^0 \sum_{i=1}^p L_i^0/\epsilon^2$, potentially leading to improvements in certain settings (depending on the relationship between the sequences $\{L_i^0\}$ and $\{L_i^1\}$–see Remark 4). However, this introduces a dependence on $L_{\max}^1 := \max_{i=1,\dots,p} L_i^1$ in the second term. Empirically, we find that $L_i^0 \approx 0$ across all layers (see Section 5), making the first term vanish in both bounds. In this case, the rate (8) is clearly superior, replacing the worst-case constant $L_{\max}^1$ with the more favorable harmonic mean.

When $p = 1$, our rates match the best-known complexity for finding a stationary point of (L^0, L^1)-smooth functions, $\mathcal{O}\left(L^0\Delta^0/\epsilon^2 + L^1\Delta^0/\epsilon\right)$, as established by Vankov et al. (2025) for the Gradient Method. While no prior work has analyzed deterministic Gluon under general (L^0, L^1)-smoothness, there exist analyses under classical L-smoothness, treating the parameters as a single vector. The analysis by Kovalev (2025) guarantees convergence in $K = \lceil 6L\Delta^0/\epsilon^2 \rceil$ iterations. The same bound appears in Li & Hong (2025) and Pethick et al. (2025b) (by setting $\sigma^2 = 0$). Since for $p = 1$, L-smoothness implies Assumption 1 with $L^1 = 0$ (Lemma 2), our rates match these prior results up to a constant factor. Thus, even in the smooth setting, our bounds are as tight as those derived specifically for it.

[5] Weight sharing refers to the practice of using the same parameters (weights) for different parts of a model, rather than allowing each part to have its own unique parameters.

However, the real strength of our guarantees lies in their broader applicability. Our analysis is much more general than prior studies, as it extends beyond standard smoothness–allowing $L_i^1 > 0$ introduces additional terms that drive the accelerated convergence enabled by (L^0, L^1)-smoothness. This richer model is *essential for explaining the empirical speedup* of methods like Muon, and much more accurately reflects the geometry of neural network loss surfaces. Indeed, as we demonstrate in Section 5, the assumption typically holds with $L_i^0 \approx 0$ and $L_i^1 > 0$.

Practical radii t_i^k. Unlike previous analyses (Kovalev, 2025; Li & Hong, 2025; Pethick et al., 2025b), which prescribe impractically small constant radii proportional to ϵ, our framework allows t_i^k to be *adaptive* to the loss landscape. Therefore, t_i^k can be larger early in training when $\|\nabla_i f(X^k)\|_{(i)\star}$ is large and gradually shrink as the gradient norm decreases. In the special case when $L_i^0 \approx 0$ (as observed empirically), $t_i^k \approx 1/L_i^1$, which is substantially larger than the radii dictated by earlier analyses. Crucially, as shown in Section 5.1, our adaptive stepsizes closely match those that yield state-of-the-art empirical performance identified by Pethick et al. (2025b) through hyperparameter tuning. This alignment demonstrates that *principled, theory-driven stepsize selection could substantially reduce the need for costly manual tuning*.

4.3 Stochastic case

In practice, computing full gradients is often infeasible due to the scale of modern ML problems. We therefore turn to the practical Gluon (Algorithm 1), a stochastic variant of Algorithm 2 that operates with noisy gradient estimates available through a stochastic gradient oracle ∇f_ξ, $\xi \sim \mathcal{D}$.

Assumption 2. *The stochastic gradient estimator $\nabla f_\xi : \mathcal{S} \mapsto \mathcal{S}$ is unbiased and has bounded variance. That is, $\mathbb{E}_{\xi\sim\mathcal{D}}[\nabla f_\xi(X)] = \nabla f(X)$ for all $X \in \mathcal{S}$ and there exists $\sigma \geq 0$ such that $\mathbb{E}_{\xi\sim\mathcal{D}}\left[\|\nabla_i f_\xi(X) - \nabla_i f(X)\|_2^2\right] \leq \sigma^2$ for all $X \in \mathcal{S}$, $i = 1, \ldots, p$.*

Note that the choice of norm in Assumption 2 is not restrictive: in finite-dimensional spaces, all norms are equivalent, so variance bounds remain valid up to a constant factor when compared to those based on any non-Euclidean norm. The following result establishes the convergence properties.

Theorem 2. *Let Assumptions 1 and 2 hold and fix $\varepsilon > 0$. Let $X^0, \ldots, X^{K-1}$ be the iterates of Gluon (Algorithm 1) run with $\beta^k = 1 - (k+1)^{-1/2}$, $t_i^k = t_i(k+1)^{-3/4}$ for some $t_i > 0$, and $M_i^0 = \nabla_i f_{\xi^0}(X^0)$. Then*

$$\min_{k=0,\ldots,K-1} \sum_{i=1}^{p} \frac{1}{12L_i^1} \mathbb{E}\left[\|\nabla_i f(X^k)\|_{(i)\star}\right] \lesssim \frac{\Delta^0}{K^{1/4}} + \frac{1}{K^{1/4}} \sum_{i=1}^{p} \left[\frac{\sigma}{L_i^1} + \frac{L_i^0}{(L_i^1)^2}\right], \tag{9}$$

where $\Delta^0 := f(X^0) - f^{\inf}$ and the notation $\lesssim$ omits numerical constants and logarithmic factors.

For $p = 1$, our rate in (9) recovers the complexity for finding a stationary point of (L^0, L^1)-smooth functions established by Hübler et al. (2024) for normalized SGD with momentum. When $p \geq 1$, compared to existing guarantees for Gluon, our Theorem 2 operates under the significantly more general Assumption 1 and uniquely supports training with larger, non-constant stepsizes $t_i^k \propto k^{-3/4}$. In contrast, prior analyses prescribe constant, vanishingly small stepsizes $t_i^k \equiv t_i \propto K^{-3/4}$, tied to the *total* number of iterations K (see Table 1).

5 Experiments

Below, we highlight selected experimental results for the unScion optimizer, a special case of Gluon (see Appendix D.1). Additional details and further experiments are provided in Appendix F.[6]

5.1 Training NanoGPT on FineWeb

In the first set of experiments, we aim to verify layer-wise (L^0, L^1)-smoothness (Assumption 1). To this end, we train the `NanoGPT` model with 124M parameters on the `FineWeb` dataset, leveraging two open-source GitHub repositories (Jordan et al., 2024a; Pethick et al., 2025a). We use the unScion optimizer, i.e., Gluon with the norm choices as in (6). We adopt the hyperparameters from Pethick et al. (2025b, Table 7), mapping their values $\gamma = 0.00036$, $\rho_2 = 50$, and $\rho_3 = 3000$ into our notation as follows: $t_i^k \equiv \gamma\rho_2 = 0.018$ for $i = 1, \ldots, p-1$ (corresponding to the transformer block layers), and $t_p^k \equiv \gamma\rho_3 = 1.08$ (token embeddings and output projections, due to weight sharing). We set the number of warmdown iterations to 0 to keep the learning rates constant throughout training.

[6] Code for all experiments is available here.

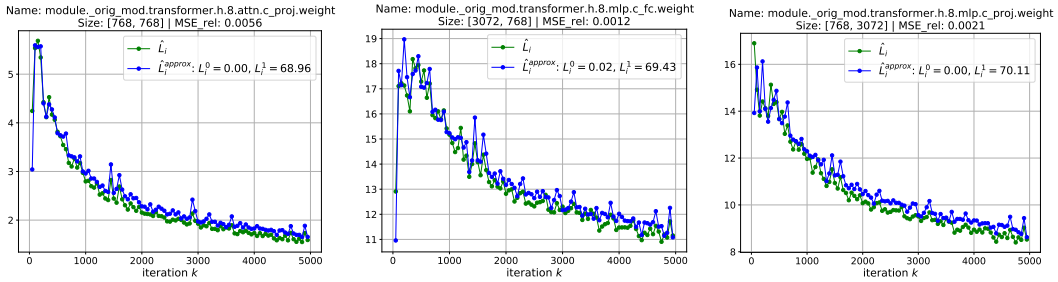

Figure 2: Validation of Assumption 1 for the 8th transformer block in `NanoGPT-124M` along training trajectories of unScion.

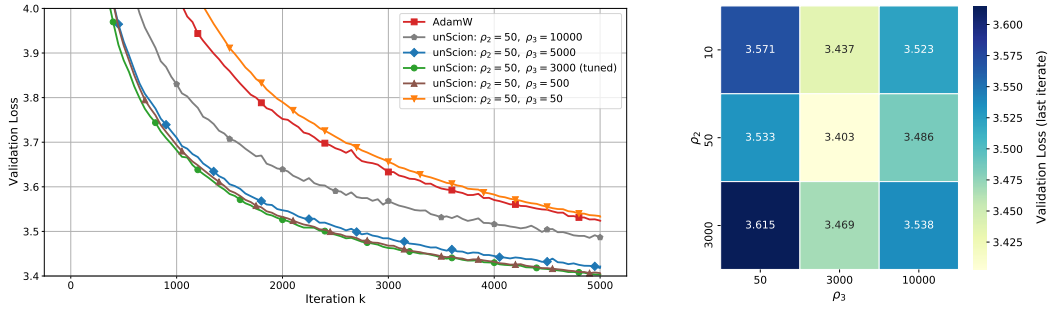

(a) (b)

Figure 3: (a) Validation curves for AdamW and unScion with varying ρ_3 values; (b) Heatmap of validation loss from the last iteration of unScion across different combinations of ρ_2 and ρ_3.

The model is trained for 5,000 iterations in accordance with the Chinchilla scaling laws to ensure compute-optimal training. In Figures 2, 5, 6, we plot the estimated *trajectory smoothness* as a function of the iteration index k

$$\hat{L}_i[k] := \|\nabla_i f_{\xi^{k+1}}(X^{k+1}) - \nabla_i f_{\xi^k}(X^k)\|_{(i)\star} / \|X_i^{k+1} - X_i^k\|_{(i)} \tag{10}$$

for parameter groups from the embedding layer and 4th and 8th transformer blocks (with similar trends observed across all blocks). We compare this to the approximation

$$\hat{L}_i^{\text{approx}}[k] := L_i^0 + L_i^1 \|\nabla_i f_{\xi^{k+1}}(X^{k+1})\|_{(i)\star},$$

where $L_i^0, L_i^1 \geq 0$ are fitted to minimize the Euclidean error between $\hat{L}_i[k]$ and $\hat{L}_i^{\text{approx}}[k]$, with hinge-like penalty on underestimation (see Appendix F.2). The close alignment between these curves implies that Assumption 1 is approximately satisfied along the training trajectories.

Effect of scaling factors. We next evaluate the impact of the learning rate scaling factors ρ_2 and ρ_3 on the performance of the unScion optimizer. For consistency, all other hyperparameters are fixed as described earlier. As a baseline, we include results obtained with the AdamW optimizer, using the hyperparameter settings from Section F.3.3. Figure 3 presents (a) validation curves for both optimizers, with varying ρ_3 in unScion, and (b) the final validation loss for unScion across different combinations of ρ_2 and ρ_3. The best performance is achieved with $\rho_2 = 50$ and $\rho_3 = 3000$, i.e., $t_i^k = 0.018$ for $i = 1, \ldots, p-1$ and $t_p^k = 1.08$.This supports the use of non-uniform scaling across layers, with larger step sizes for the embedding layer.

Additional ablation studies. In Appendix F.3.2, we present an ablation study demonstrating that specialized norms provide a better approximation of trajectory smoothness compared to the standard Euclidean norm. Appendix F.3.3 demonstrates that the layer-wise (L^0, L^1)-smoothness model also closely approximates trajectory smoothness during AdamW training. Notably, we observe a similar gap between transformer and embedding layers as with Scion, suggesting that smoothness statistics from AdamW training can guide per-layer learning rate tuning in Scion.

5.2 Training CNN on CIFAR-10

In this experiment, we further validate layer-wise (L^0, L^1)-smoothness by training a `CNN` model on the `CIFAR-10` dataset, following implementations from two open-source GitHub repositories (Jordan, 2024; Pethick et al., 2025a). The model is trained using the unScion optimizer (15) with full-batch gradients $\nabla_i f$, no momentum and no learning rate decay (results for the stochastic case are reported in Appendix F.4). Other hyperparameters are as in Pethick et al. (2025b, Table 10), except that we train for more epochs. Similar to the `NanoGPT` experiments discussed in Section 5.1, we plot the estimated (non-stochastic) trajectory smoothness $\hat{L}_i[k] := \|\nabla_i f(X^{k+1}) - \nabla_i f(X^k)\|_{(i)\star} / \|X_i^{k+1} - X_i^k\|_{(i)}$ alongside its approximation $\hat{L}_i^{\text{approx}}[k] := L_i^0 + L_i^1 \|\nabla_i f(X^{k+1})\|_{(i)\star}$ for selected parameter groups. In this experiment, we consider a simplified variant of Assumption 1, setting $L_i^0 = 0$, and estimate $L_i^1 \geq 0$ using the same procedure as in Section 5.1. Figure 4 presents the results, demonstrating that Assumption 1 is approximately satisfied along the training trajectory. When this condition holds with $L_i^0 = 0$, Theorem 1 guarantees convergence under the stepsize choice $t_i^k \equiv t_i = 1/L_i^1$. In this setting, the estimated L_i^1 values (shown in Figure 4) are $L_i^1 \approx 3$ for all parameter groups except for the classification head weights X_p, where $L_p^1 \approx 0.03$. This roughly two-orders-of-magnitude difference justifies the much larger radius t_p^k used for the head weights in the tuned configuration reported in Pethick et al. (2025b, Table 10).

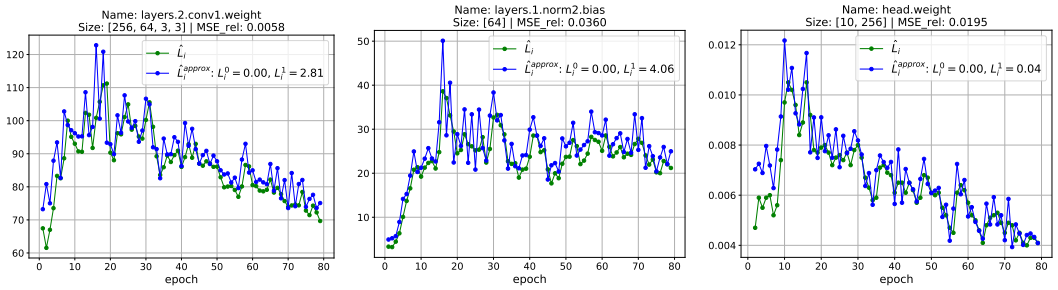

Figure 4: Validation of Assumption 1 for different groups of parameters in `CNN` along training trajectories of unScion with full-batch gradients.

6 Conclusion and Future Work

In this work, we propose Gluon, an LMO-based optimization method that recovers state-of-the-art optimizers such as Muon and Scion as special cases. We develop a principled analytical framework for layer-wise optimization based on a novel *layer-wise* (L^0, L^1)*-smoothness* assumption, which captures the anisotropic structure of modern deep networks. This assumption enables sharper and more general convergence guarantees and, unlike prior analyses, yields theoretical stepsizes that closely match those found via finetuning. Our framework thus provides *the first rigorous and practically predictive analysis of modern layer-wise optimizers*. Experiments confirm that the assumption holds approximately throughout training, reinforcing its practical relevance. Together, these results offer a refined foundation for structured optimization in deep learning.

While this work resolves two key theoretical gaps (Sections 2.1 and 2.2), it also highlights important directions for future research. Our analysis assumes exact LMO computations, whereas practical implementations use approximations (Appendix F.1). Additionally, our stochastic guarantees (Theorem 2) rely on the widely adopted bounded variance assumption, which may not hold in certain scenarios, e.g., under subsampling (Khaled & Richtárik, 2020). Finally, our support for adaptive stepsizes is currently restricted to the deterministic setting. While they also perform well empirically in the stochastic regime (Section 5.1), a complete theoretical justification remains an open challenge.

In summary, although we make substantial progress by closing the two most critical gaps–establishing a realistic generalized smoothness model and aligning analysis with actual implementations–no single work can exhaust the subject. The field remains open, with many fruitful directions left to pursue.

REFERENCES

Lukas Balles, Fabian Pedregosa, and Nicolas Le Roux. The geometry of Sign Gradient Descent, 2020. URL https://arxiv.org/abs/2002.08056. (Cited on page 6 and 18)

Jeremy Bernstein and Laker Newhouse. Modular duality in deep learning. *arXiv preprint arXiv:2410.21265*, 2024a. URL https://arxiv.org/abs/2410.21265. (Cited on page 17)

Jeremy Bernstein and Laker Newhouse. Old optimizer, new norm: An anthology. In *OPT 2024: Optimization for Machine Learning*, 2024b. URL https://arxiv.org/abs/2409.20325. (Cited on page 14 and 18)

Jeremy Bernstein, Yu-Xiang Wang, Kamyar Azizzadenesheli, and Animashree Anandkumar. signSGD: Compressed optimisation for non-convex problems. In *International Conference on Machine Learning*, pp. 560–569. PMLR, 2018. URL https://arxiv.org/abs/1802.04434. (Cited on page 14)

Aleksandr Beznosikov, Samuel Horváth, Peter Richtárik, and Mher Safaryan. On biased compression for distributed learning. *Journal of Machine Learning Research*, 24(276):1–50, 2023. (Cited on page 24)

Michael Crawshaw, Mingrui Liu, Francesco Orabona, Wei Zhang, and Zhenxun Zhuang. Robustness to unbounded smoothness of generalized signSGD. *Advances in neural information processing systems*, 35:9955–9968, 2022. URL https://arxiv.org/abs/2208.11195. (Cited on page 3 and 14)

Yury Demidovich, Grigory Malinovsky, Igor Sokolov, and Peter Richtárik. A guide through the zoo of biased sgd. *Advances in Neural Information Processing Systems*, 36:23158–23171, 2023. (Cited on page 24)

Marguerite Frank and Philip Wolfe. An algorithm for quadratic programming. *Naval Research Logistics Quarterly*, 3(1-2):95–110, 1956. URL https://onlinelibrary.wiley.com/doi/abs/10.1002/nav.3800030109. (Cited on page 1 and 14)

Eduard Gorbunov, Nazarii Tupitsa, Sayantan Choudhury, Alen Aliev, Peter Richtárik, Samuel Horváth, and Martin Takáč. Methods for convex (L_0, L_1)-smooth optimization: Clipping, acceleration, and adaptivity. In *The Thirteenth International Conference on Learning Representations*, 2025. URL https://arxiv.org/abs/2409.14989. (Cited on page 14)

Kaja Gruntkowska, Hanmin Li, Aadi Rane, and Peter Richtárik. The Ball-Proximal (="Broximal") Point Method: a new algorithm, convergence theory, and applications. *arXiv preprint arXiv:2502.02002*, 2025. URL https://arxiv.org/abs/2502.02002. (Cited on page 17)

Florian Hübler, Junchi Yang, Xiang Li, and Niao He. Parameter-agnostic optimization under relaxed smoothness. In *International Conference on Artificial Intelligence and Statistics*, pp. 4861–4869. PMLR, 2024. URL https://arxiv.org/abs/2311.03252. (Cited on page 7, 14, 16, and 29)

Martin Jaggi. Revisiting frank-wolfe: Projection-free sparse convex optimization. In *International conference on machine learning*, pp. 427–435. PMLR, 2013. (Cited on page 14)

Ruichen Jiang, Devyani Maladkar, and Aryan Mokhtari. Convergence analysis of adaptive gradient methods under refined smoothness and noise assumptions. *arXiv preprint arXiv:2406.04592*, 2024. URL https://arxiv.org/abs/2406.04592. (Cited on page 14)

Keller Jordan. Cifar-10 airbench. https://github.com/KellerJordan/cifar10-airbench, 2024. GitHub repository. (Cited on page 9 and 33)

Keller Jordan, Jeremy Bernstein, Ben Rappazzo, B. Vlado, Y. Jiacheng, F. Cesista, and B. Koszarsky. Modded-nanoGPT: Speedrunning the nanoGPT baseline. https://github.com/KellerJordan/modded-nanogpt, 2024a. GitHub repository. Additional contributors: @fern-bear.bsky.social, @Grad62304977. (Cited on page 3, 7, and 33)

Keller Jordan, Yuchen Jin, Vlado Boza, Jiacheng You, Franz Cesista, Laker Newhouse, and Jeremy Bernstein. Muon: An optimizer for hidden layers in neural networks, 2024b. URL https://kellerjordan.github.io/posts/muon/. (Cited on page 1, 3, 6, 14, 18, and 33)

Hamed Karimi, Julie Nutini, and Mark Schmidt. Linear convergence of gradient and proximal-gradient methods under the Polyak-Łojasiewicz condition, 2020. URL https://arxiv.org/abs/1608.04636. (Cited on page 22)

Ahmed Khaled and Peter Richtárik. Better theory for SGD in the nonconvex world. *arXiv preprint arXiv:2002.03329*, 2020. URL https://arxiv.org/abs/2002.03329. (Cited on page 9 and 24)

Diederik P Kingma and Jimmy Ba. Adam: A method for stochastic optimization. In *International Conference on Learning Representations*, 2015. URL https://arxiv.org/abs/1412.6980. (Cited on page 1)

Dmitry Kovalev. Understanding gradient orthogonalization for deep learning via non-Euclidean trust-region optimization, 2025. URL https://arxiv.org/abs/2503.12645. (Cited on page 2, 3, 5, 6, 7, 14, and 17)

Tim Large, Yang Liu, Minyoung Huh, Hyojin Bahng, Phillip Isola, and Jeremy Bernstein. Scalable optimization in the modular norm. In *The Thirty-eighth Annual Conference on Neural Information Processing Systems*, 2024. URL https://arxiv.org/abs/2405.14813. (Cited on page 17)

Jiaxiang Li and Mingyi Hong. A note on the convergence of Muon and further, 2025. URL https://arxiv.org/abs/2502.02900. (Cited on page 2, 3, 5, 6, 7, and 14)

Chaoyue Liu, Libin Zhu, and Mikhail Belkin. Loss landscapes and optimization in over-parameterized non-linear systems and neural networks. *Applied and Computational Harmonic Analysis*, 59, 01 2022. doi: 10.1016/j.acha.2021.12.009. URL https://arxiv.org/abs/2003.00307. (Cited on page 22)

Jingyuan Liu, Jianlin Su, Xingcheng Yao, Zhejun Jiang, Guokun Lai, Yulun Du, Yidao Qin, Weixin Xu, Enzhe Lu, Junjie Yan, et al. Muon is scalable for LLM training. *arXiv preprint arXiv:2502.16982*, 2025. URL https://arxiv.org/abs/2502.16982. (Cited on page 1)

Yuxing Liu, Rui Pan, and Tong Zhang. AdaGrad under anisotropic smoothness, 2024. URL https://arxiv.org/abs/2406.15244. (Cited on page 4 and 14)

Ilya Loshchilov and Frank Hutter. Decoupled weight decay regularization. In *International Conference on Learning Representations*, 2019. URL https://arxiv.org/abs/1711.05101. (Cited on page 1)

Yu Nesterov. Efficiency of coordinate descent methods on huge-scale optimization problems. *SIAM Journal on Optimization*, 22(2):341–362, 2012. URL https://epubs.siam.org/doi/10.1137/100802001. (Cited on page 14)

Thomas Pethick, Wanyun Xie, Kimon Antonakopoulos, Zhenyu Zhu, Antonio Silveti-Falls, and Volkan Cevher. Scion. https://github.com/LIONS-EPFL/scion.git, 2025a. GitHub repository. (Cited on page 3, 7, 9, and 33)

Thomas Pethick, Wanyun Xie, Kimon Antonakopoulos, Zhenyu Zhu, Antonio Silveti-Falls, and Volkan Cevher. Training deep learning models with norm-constrained LMOs. *arXiv preprint arXiv:2502.07529*, 2025b. URL https://arxiv.org/abs/2502.07529. (Cited on page 1, 2, 3, 4, 5, 6, 7, 9, 14, 17, 18, 19, 36, and 37)

Sebastian Pokutta. The Frank-Wolfe algorithm: a short introduction. *Jahresbericht der Deutschen Mathematiker-Vereinigung*, 126(1):3–35, 2024. URL https://arxiv.org/abs/2311.05313. (Cited on page 1)

Peter Richtárik and Martin Takáč. Iteration complexity of randomized block-coordinate descent methods for minimizing a composite function. *Mathematical Programming*, 144(1):1–38, 2014. URL https://arxiv.org/abs/1107.2848. (Cited on page 14)

Ishaan Shah, Anthony M Polloreno, Karl Stratos, Philip Monk, Adarsh Chaluvaraju, Andrew Hojel, Andrew Ma, Anil Thomas, Ashish Tanwer, Darsh J Shah, et al. Practical efficiency of Muon for pretraining. *arXiv preprint arXiv:2505.02222*, 2025. URL https://arxiv.org/abs/2505.02222. (Cited on page 2)

Daniil Vankov, Anton Rodomanov, Angelia Nedich, Lalitha Sankar, and Sebastian U Stich. Optimizing (L_0, L_1)-smooth functions by gradient methods. In *The Thirteenth International Conference on Learning Representations*, 2025. URL https://arxiv.org/abs/2410.10800. (Cited on page 6, 14, and 18)

Ashia C Wilson, Rebecca Roelofs, Mitchell Stern, Nati Srebro, and Benjamin Recht. The marginal value of adaptive gradient methods in machine learning. *Advances in neural information processing systems*, 30, 2017. URL https://arxiv.org/abs/1705.08292. (Cited on page 1)

Shuo Xie, Mohamad Amin Mohamadi, and Zhiyuan Li. Adam exploits ℓ_∞-geometry of loss landscape via coordinate-wise adaptivity. *arXiv preprint arXiv:2410.08198*, 2024. URL https://arxiv.org/abs/2410.08198. (Cited on page 14)

Adams Wei Yu, Lei Huang, Qihang Lin, Ruslan Salakhutdinov, and Jaime Carbonell. Block-normalized gradient method: An empirical study for training deep neural network, 2018. URL https://openreview.net/forum?id=ry831QWAb. (Cited on page 6 and 18)

Dingzhi Yu, Wei Jiang, Yuanyu Wan, and Lijun Zhang. Mirror descent under generalized smoothness. *arXiv preprint arXiv:2502.00753*, 2025. (Cited on page 14)

Jingzhao Zhang, Tianxing He, Suvrit Sra, and Ali Jadbabaie. Why gradient clipping accelerates training: A theoretical justification for adaptivity. In *International Conference on Learning Representations*, 2020. URL https://arxiv.org/abs/1905.11881. (Cited on page 3, 4, 5, and 14)

Difan Zou, Yuan Cao, Yuanzhi Li, and Quanquan Gu. Understanding the generalization of Adam in learning neural networks with proper regularization. *arXiv preprint arXiv:2108.11371*, 2021. URL https://arxiv.org/abs/2108.11371. (Cited on page 1)

APPENDIX

CONTENTS

A Related works

Generalized Smoothness. The classical L-smoothness assumption, where the gradient is Lipschitz continuous with a global constant L, often fails to accurately capture the complex geometry of loss landscapes in deep learning (Crawshaw et al., 2022; Zhang et al., 2020). To address this, Zhang et al. (2020) introduced the (L^0, L^1)-smoothness condition, empirically observing in language model experiments that a bound of the form $\|\nabla^2 f(x)\| \leq L_0 + L_1\|\nabla f(x)\|$ better described the Hessian norm behavior. Subsequent works have analyzed standard optimization algorithms under this generalized smoothness framework. For instance, Gorbunov et al. (2025) and Vankov et al. (2025) provided convergence analyses for the Gradient Method. Hübler et al. (2024) analyzed Normalized SGD with momentum in a parameter-agnostic setting under (L^0, L^1)-smoothness. Yu et al. (2025) proposed non-Euclidean generalized smoothness and established convergence rates for mirror-descent-type methods. Our work extends this line by incorporating (L^0, L^1)-smoothness into a *layer-wise* context using arbitrary norms, an approach that is particularly well-suited for the LMO-based optimizers we study.

Anisotropic Smoothness. Recognizing the heterogeneous nature of parameters in large models, researchers have explored anisotropic smoothness conditions, where smoothness constants can vary across different dimensions or parameter blocks. Early work in this direction includes coordinate-wise Lipschitz continuity for coordinate descent methods (Nesterov, 2012; Richtárik & Takáč, 2014). More recently, Bernstein et al. (2018) analyzed signSGD under a weaker notion of coordinate-wise smoothness. Crawshaw et al. (2022) further developed this by analyzing Generalized signSGD under a generalized coordinate-wise smoothness assumption, highlighting that different parameter groups can exhibit vastly different geometries. Jiang et al. (2024) focused on Adagrad's analysis under coordinate-wise smoothness and established lower bounds for SGD, underscoring the benefits of adaptivity. Liu et al. (2024) proposed "Anisotropic (L^0, L^1)-smoothness" (a vector version of (L_0, L_1)-smoothness applied coordinate-wise) and demonstrated Adagrad's provable advantages over SGD in this setting. Xie et al. (2024) also leveraged anisotropic smoothness concepts in their convergence analysis of Adam. Our work contributes by defining and analyzing *layer-wise* (L^0, L^1)-*smoothness*, which combines the benefits of the generalized smoothness model with a structured, anisotropic perspective tailored to the layer-block architecture of neural networks and compatible with arbitrary layer-specific norms. This framework is essential for understanding LMO-based methods like Muon and Scion.

LMO-based Optimizers. The optimizers Muon (Jordan et al., 2024b) and Scion (Pethick et al., 2025b) represent a recent class of methods that have shown strong empirical performance in deep learning. Muon was initially introduced as an effective empirical method, with its update rule for hidden layers inspired by ideas from Bernstein & Newhouse (2024b). Subsequently, Pethick et al. (2025b) (authors of Scion) explicitly connected these types of updates to the Frank-Wolfe (FW) framework (Frank & Wolfe, 1956; Jaggi, 2013), proposing the use of layer-specific norms within an LMO-based update rule. These methods perform updates by solving, for each layer, a linear minimization problem over a norm ball centered at the current iterate. Prior theoretical analyses of these optimizers (Kovalev, 2025; Li & Hong, 2025; Pethick et al., 2025b) have relied on standard L-smoothness and analyzed a simplified global update. Our work provides the first convergence guarantees for these methods under the more realistic layer-wise (L_0, L_1)-smoothness, directly addressing their practical layer-wise nature and leveraging the geometric insights offered by LMOs over general norms.

Acknowledgments

The authors used large language models (LLMs) during the preparation of this paper to assist with grammar, wording, and code implementation. No LLMs were used to write scientific content, or search for citations or related work. This is in accordance with two main LLM-related policies.

B AUXILIARY LEMMAS

Lemma 1. *Let $f : \mathcal{S} \mapsto \mathbb{R}$ satisfy Assumption 1. Then, for any $X, Y \in \mathcal{S}$, we have*

$$|f(Y) - f(X) - \langle \nabla f(X), Y - X\rangle| \leq \sum_{i=1}^{p} \frac{L_i^0 + L_i^1 \|\nabla_i f(X)\|_{(i)\star}}{2} \|Y_i - X_i\|_{(i)}^2.$$

Proof. For all $X, Y \in \mathcal{S}$ we have

$$\begin{aligned} f(Y) &= f(X) + \int_0^1 \langle \nabla f(X + \tau(Y - X)), Y - X\rangle \, d\tau \\ &= f(X) + \langle \nabla f(X), Y - X\rangle + \int_0^1 \langle \nabla f(X + \tau(Y - X)) - \nabla f(X), Y - X\rangle \, d\tau. \end{aligned}$$

Therefore, using the Cauchy-Schwarz inequality and Assumption 1, we obtain

$$\begin{aligned} &|f(Y) - f(X) - \langle \nabla f(X), Y - X\rangle| \\ &\leq \left| \int_0^1 \sum_{i=1}^{p} \langle \nabla_i f(X + \tau(Y - X)) - \nabla_i f(X), Y_i - X_i\rangle_{(i)} \, d\tau \right| \\ &\leq \int_0^1 \sum_{i=1}^{p} \left| \langle \nabla_i f(X + \tau(Y - X)) - \nabla_i f(X), Y_i - X_i\rangle_{(i)} \right| d\tau \\ &\leq \int_0^1 \sum_{i=1}^{p} \|\nabla_i f(X + \tau(Y - X)) - \nabla_i f(X)\|_{(i)\star} \|Y_i - X_i\|_{(i)} d\tau \\ &\leq \int_0^1 \sum_{i=1}^{p} \tau \left(L_i^0 + L_i^1 \|\nabla_i f(X)\|_{(i)\star}\right) \|Y_i - X_i\|_{(i)}^2 d\tau \\ &= \sum_{i=1}^{p} \frac{L_i^0 + L_i^1 \|\nabla_i f(X)\|_{(i)\star}}{2} \|Y_i - X_i\|_{(i)}^2. \end{aligned}$$

□

Lemma 2. *Suppose that f is L-smooth with respect to the norm defined in (11), i.e.,*

$$\|\nabla f(X) - \nabla f(Y)\|_{\max\star} \leq L \|X - Y\|_{\max},$$

where $X = [X_1, \ldots, X_p]$ and $Y = [Y_1, \ldots, Y_p]$ with $X_i, Y_i \in \mathcal{S}_i$. Then Assumption 1 holds with $L_i^0 \leq L$ and $L_i^1 = 0$ for all $i = 1, \ldots, p$.

Proof. L-smoothness and the definition of the norm give

$$\sum_{i=1}^{p} \|\nabla_i f(X) - \nabla_i f(Y)\|_{(i)\star} \leq L \max\left\{ \|X_1 - Y_1\|_{(1)}, \ldots, \|X_p - Y_p\|_{(p)} \right\}$$

for all $X, Y \in \mathcal{S}$. In particular, choosing $X = [X_1, \ldots, X_p]$ and $Y = [X_1, \ldots, X_{j-1}, Y_j, X_{j+1}, \ldots X_p]$, we have

$$\|\nabla_j f(X) - \nabla_j f(Y)\|_{(j)\star} \leq \sum_{i=1}^{p} \|\nabla_i f(X) - \nabla_i f(Y)\|_{(i)\star} \leq L \|X_j - Y_j\|_{(j)}$$

for any $j \in \{1, \ldots, p\}$, proving the claim. □

Lemma 3. *Suppose that $x_1, \ldots, x_p, y_1, \ldots, y_p \in \mathbb{R}$, $\max_{i\in[p]} |x_i| > 0$ and $z_1, \ldots, z_p > 0$. Then*

$$\sum_{i=1}^{p} \frac{y_i^2}{z_i} \geq \frac{\left(\sum_{i=1}^{p} x_i y_i\right)^2}{\sum_{i=1}^{p} z_i x_i^2}.$$

Proof. Cauchy-Schwarz inequality gives

$$\left(\sum_{i=1}^{p} x_i y_i\right)^2 = \left(\sum_{i=1}^{p} \frac{y_i}{\sqrt{z_i}} \sqrt{z_i} x_i\right)^2 \leq \left(\sum_{i=1}^{p} \frac{y_i^2}{z_i}\right) \left(\sum_{i=1}^{p} z_i x_i^2\right).$$

Rearranging, we obtain the result. □

Lemma 4 (Technical Lemma 10 by Hübler et al. (2024))**.** *Let $q \in (0, 1)$, $p \geq 0$, and $p \geq q$. Further, let $a, b \in \mathbb{N}_{\geq 2}$ with $a \leq b$. Then*

$$\sum_{k=a-1}^{b-1} (1+k)^{-p} \prod_{\tau=a-1}^{k} \left(1 - (\tau+1)^{-q}\right) \leq (a-1)^{q-p} \exp\left(\frac{a^{1-q} - (a-1)^{1-q}}{1-q}\right).$$

Lemma 5 (Technical Lemma 11 by Hübler et al. (2024))**.** *Let $t > 0$ and for $k \in \mathbb{N}_{\geq 0}$, set $\beta^k = 1 - (k+1)^{-1/2}$, $t^k = t(k+1)^{-3/4}$, $t > 0$. Then, for all $K \in \mathbb{N}_{\geq 1}$ the following inequalities hold:*

(i) $\sum_{k=0}^{K-1} t^k \sqrt{\sum_{\tau=0}^{k} (1-\beta^\tau)^2 \prod_{\kappa=\tau+1}^{k} (\beta^\kappa)^2} \leq t\left(\frac{7}{2} + \sqrt{2e^2}\log(K)\right)$,

(ii) $\sum_{k=0}^{K-1} t^k \sum_{\tau=1}^{k} t^\tau \prod_{\kappa=\tau}^{k} \beta^\kappa \leq 7t^2\,(3 + \log(K))$.

Proof. This is a direct consequence of Lemma 11 by Hübler et al. (2024). To obtain *(ii)*, it suffices to take the limit as $L^1 \to 0$ in statement *(ii)* of part (b). □

C Remarks on the theoretical results

C.1 Note on radii and stepsizes

It is known (see, e.g., Gruntkowska et al. (2025, Theorem D.1), who establish this for $\mathcal{S} = \mathbb{R}^d$ under Euclidean norms; the extension to general normed vector spaces is entirely analogous) that if g is a convex function, then the solution to the problem

$$\arg\min_{X \in \mathcal{B}^k} g(X)$$

lies on the boundary of the ball $\mathcal{B}^k := \{X \in \mathcal{S} : \|X - X^k\| \leq t^k\}$ (unless $\mathcal{B}^k \cap \arg\min_{X \in \mathcal{S}} g(X) \neq \emptyset$, that is, the ball intersects the set of minimizers of g).

This applies directly to the LMO subproblem solved at each iteration of Gluon in (1), since the objective $\langle M_i^k, X_i \rangle_{(i)}$ is linear in X_i, and hence convex. In other words, each LMO step moves the iterate from the center of the ball X_i^k to a new point X_i^{k+1} located on the boundary of $\mathcal{B}_i^k$, effectively traversing a distance of t_i^k at each step. For this reason, we use the terms *radius*, *stepsize*, and *learning rate* interchangeably.

C.2 Note on prior analyses

As presented, prior convergence results do not directly apply to the algorithms used in practice. However, there is a workaround. Specifically, some of the existing convergence guarantees (Kovalev, 2025; Pethick et al., 2025b) expressed in terms of the flat vector x are transferable to the structured parameters $X = [X_1, \ldots, X_l] \in \mathcal{S}$ by employing the max-norm (Bernstein & Newhouse, 2024a; Large et al., 2024), defined as

$$\|X\|_{\max} := \max\left\{\|X_1\|_{(1)}, \ldots, \|X_p\|_{(p)}\right\}, \tag{11}$$

with corresponding dual norm $\|Y\|_{\max\star} = \sup_{\|X\|_{\max} \leq 1} \langle X, Y \rangle = \sum_{i=1}^p \|Y_i\|_{(i)\star}$. Nevertheless, these works do not make this connection explicit, and an additional layer of analysis is required to ensure the guarantees meaningfully extend to the structured practical setting. Even if such a translation was attempted, the global treatment introduces serious practical limitations. For example, real-world training pipelines tune parameters on a per-layer basis, reflecting the heterogeneous structure of deep networks. Max-norm-based guarantees overlook this variability and offer no mechanism for per-layer control in hyperparameter selection.

Algorithm 2 Deterministic Adaptive Layer-Wise LMO-based Optimizer

Input: Initial model parameters $X^0 = [X_1^0, \ldots, X_p^0] \in \mathcal{S}$
for $k = 0, 1, \ldots, K-1$ **do**
  for $i = 1, 2, \ldots, p$ **do**
    Choose adaptive stepsize/radius $t_i^k > 0$ for layer i
    Update parameters for layer i via LMO over $\mathcal{B}_i^k := \{X_i \in \mathcal{S}_i : \|X_i - X_i^k\|_{(i)} \leq t_i^k\}$:

$$X_i^{k+1} = \mathrm{LMO}_{\mathcal{B}_i^k}\left(\nabla_i f(X^k)\right) := \arg\min_{X_i \in \mathcal{B}_i^k} \langle \nabla_i f(X^k), X_i \rangle_{(i)} \tag{12}$$

  end for
  Update full vector: $X^{k+1} = [X_1^{k+1}, \ldots, X_p^{k+1}]$
end for

D Deterministic case

We begin by considering the deterministic counterpart of Gluon, as formalized in Algorithm 2. We first review several existing algorithms that fall within this framework (Appendix D.1), followed by a proof of Theorem 1 (Appendix D.2). Finally, we present an additional convergence guarantee under the layer-wise Polyak-Łojasiewicz (PŁ) condition (Appendix D.3).

D.1 Special cases of the LMO framework

As outlined in Section 4.1, deterministic Gluon encompasses a general class of algorithms, parameterized by the choice of norms $\|\cdot\|_{(i)}$ in the LMO. We now provide a more detailed discussion of the most notable special cases.

Layer-wise normalized GD (Yu et al., 2018). Let $\|\cdot\|_{(i)} = \|\cdot\|_{2\to 2}$ for each parameter group and assume that $n_i = 1$ for all $i = 1, \ldots, p$. In this case, the spectral norm reduces to the standard Euclidean norm $\|\cdot\|_2$, yielding the update rule

$$X_i^{k+1} = X_i^k - t_i^k \frac{\nabla_i f(X^k)}{\|\nabla_i f(X^k)\|_2}, \quad i = 1, \ldots, p,$$

which corresponds to layer-wise normalized GD. With a suitable choice of t_i^k (see Theorem 1), the method can also recover the Gradient Method for (L^0, L^1)-smooth functions (Vankov et al., 2025).

Layer-wise signGD (Balles et al., 2020). Suppose that $\|\cdot\|_{(i)} = \|\cdot\|_{1\to\infty}$ for each parameter group, with $n_i = 1$ for all $i = 1, \ldots, p$. Then, $\|\cdot\|_{1\to\infty}$ reduces to $\|\cdot\|_\infty$, and the update becomes

$$X_i^{k+1} = X_i^k - t_i^k \mathrm{sign}\left(\nabla_i f(X^k)\right), \quad i = 1, \ldots, p,$$

where the sign function is applied element-wise. This is equivalent to layer-wise signGD.

Muon (Jordan et al., 2024b). Here, the spectral norm $\|\cdot\|_{2\to 2}$ is used for all parameter groups, without restrictions on n_i. In this case, it can be shown that (12) is equivalent to

$$X_i^{k+1} = X_i^k - t_i^k U_i^k \left(V_i^k\right)^\top, \quad i = 1, \ldots, p, \tag{13}$$

where $\nabla_i f(X^k) = U_i^k \Sigma_i^k \left(V_i^k\right)^\top$ is the singular value decomposition (Bernstein & Newhouse, 2024b). This is exactly the per-layer deterministic version of the Muon optimizer. In practical LLM training, a more general variant of (13) incorporating stochasticity and momentum is applied to the intermediate layers, while the input and output layers are optimized using other methods.

Unconstrained Scion (Pethick et al., 2025b). We can also recover two variants of unScion introduced by Pethick et al. (2025b): one for training LLMs on next-token prediction, and another for training CNNs for image classification.

- **Training LLMs.** Define the norms $\|\cdot\|_{(i)}$ as follows: for $i = 1, \ldots, p-1$, corresponding to weight matrices of transformer blocks, set $\|\cdot\|_{(i)} = \sqrt{n_i/m_i}\|\cdot\|_{2\to 2}$, and for the last

group X_p, representing the embedding and output layers (which coincide under the weight sharing regime considered here), let $\|\cdot\|_{(p)} = n_p\|\cdot\|_{1\to\infty}$. In this case, (12) becomes

$$\begin{aligned} X_i^{k+1} &= X_i^k - t_i^k\sqrt{\frac{m_i}{n_i}}U_i^k\left(V_i^k\right)^\top, \quad i = 1,\ldots,p-1, \\ X_p^{k+1} &= X_p^k - \frac{t_p^k}{n_p}\operatorname{sign}\left(\nabla_p f(X^k)\right), \end{aligned} \tag{14}$$

where $\nabla_i f(X^k) = U_i^k\Sigma_i^k\left(V_i^k\right)^\top$ is the singular value decomposition. This is equivalent to deterministic layer-wise unScion optimizer without momentum. A more general variant, incorporating stochasticity and momentum and applied to all layers, was shown by Pethick et al. (2025b) to outperform Muon on LLM training tasks.

- **Training CNNs.** The main difference in the CNN setting is the presence of not only 2D weight matrices, but also 1D bias vectors and 4D convolutional kernels parameters. Biases are 1D tensors of shape $\mathbb{R}^{C_i^{out}}$, for which we use scaled Euclidean norms. Convolutional parameters (conv) are 4D tensors with shapes $\mathbb{R}^{C_i^{out}\times C_i^{in}\times k\times k}$, where C_i^{out} and C_i^{in} denote the number of output and input channels, and k is the kernel size. To compute norms, we reshape each 4D tensor to a 2D matrix of shape $\mathbb{R}^{C_i^{out}\times C_i^{in}k^2}$, and then apply a scaled $\|\cdot\|_{2\to2}$ norm. This yields the norm choices $\|\cdot\|_{(i)} = \sqrt{1/C_i^{out}}\|\cdot\|_2$ for biases, $\|\cdot\|_{(i)} = k^2\sqrt{C_i^{in}/C_i^{out}}\|\cdot\|_{2\to2}$ for conv, and $\|\cdot\|_{(p)} = n_p\|\cdot\|_{1\to\infty}$ for the last group X_p, associated with classification head weights. Then, it can be shown that (12) is equivalent to

$$\begin{aligned} X_i^{k+1} &= X_i^k - t_i^k\sqrt{C_i^{out}}\frac{\nabla_i f(X^k)}{\|\nabla_i f(X^k)\|_2}, && \text{(for biases)}, \\ X_i^{k+1} &= X_i^k - t_i^k\frac{1}{k^2}\sqrt{\frac{C_i^{out}}{C_i^{in}}}U_i^k\left(V_i^k\right)^\top, && \text{(for conv)}, \\ X_p^{k+1} &= X_p^k - \frac{t_p^k}{n_p}\operatorname{sign}\left(\nabla_p f(X^k)\right), && \text{(for head)} \end{aligned} \tag{15}$$

where $\nabla_i f(X^k) = U_i^k\Sigma_i^k\left(V_i^k\right)^\top$ is the singular value decomposition. This corresponds to the deterministic layer-wise unScion optimizer without momentum.

D.2 Proof of Theorem 1

We now state and prove a generalization of Theorem 1.

Theorem 3. *Let Assumption 1 hold and fix $\varepsilon > 0$. Let $X^0,\ldots,X^{K-1}$ be the iterates of deterministic* Gluon *(Algorithm 2) run with stepsizes $t_i^k = \frac{\|\nabla_i f(X^k)\|_{(i)\star}}{L_i^0 + L_i^1\|\nabla_i f(X^k)\|_{(i)\star}}$. Then,*

1. *In order to reach the precision*

$$\min_{k=0,\ldots,K-1}\sum_{i=1}^p\left\|\nabla_i f(X^k)\right\|_{(i)\star} \le \epsilon,$$

it suffices to run the algorithm for

$$K = \left\lceil \frac{2\Delta^0\sum_{i=1}^p L_i^0}{\epsilon^2} + \frac{2\Delta^0 L_{\max}^1}{\epsilon}\right\rceil \tag{16}$$

iterations;

2. *In order to reach the precision*

$$\min_{k=0,\ldots,K-1}\sum_{i=1}^p\left[\frac{\frac{1}{L_i^1}}{\frac{1}{p}\sum_{j=1}^p\frac{1}{L_j^1}}\left\|\nabla_i f(X^k)\right\|_{(i)\star}\right] \le \varepsilon, \tag{17}$$

it suffices to run the algorithm for

$$K = \left\lceil \frac{2\Delta^0 \left(\sum_{i=1}^p \frac{L_i^0}{(L_i^1)^2}\right)}{\varepsilon^2 \left(\frac{1}{p}\sum_{j=1}^p \frac{1}{L_j^1}\right)^2} + \frac{2\Delta^0}{\varepsilon \left(\frac{1}{p}\sum_{j=1}^p \frac{1}{L_j^1}\right)} \right\rceil \tag{18}$$

iterations,

where $\Delta^0 := f(X^0) - \inf_{X\in\mathcal{S}} f(X)$ *and* $L_{\max}^1 := \max_{i=1,\dots,p} L_i^1$.

Remark 4. Let us compare bounds (16) and (18). Due to the reweighting of the gradient component norms in (17), the rates are not exactly equivalent. Nevertheless, both use weights that sum to p, ensuring a fair comparison. Obviously, $(1/p \sum_{j=1}^p 1/L_j^1)^{-1} \le L_{\max}^1$, so the second term in (18) is always no worse than its counterpart in (16). The comparison of the first terms, however, depends on how the sequences $\{L_i^0\}$ and $\{L_i^1\}$ relate: if larger values of L_i^0s tend to be attached to smaller values of L_i^1, then the first term in (16) improves over that in (18), while for a positive correlation the opposite is true. Indeed, in the extreme case when $L_1^0 \ge \ldots \ge L_p^0$ and $L_1^1 \le \ldots \le L_p^1$ (or the reverse ordering), Chebyshev's sum inequality implies that

$$\frac{\sum_{i=1}^p \frac{L_i^0}{(L_i^1)^2}}{\left(\frac{1}{p}\sum_{j=1}^p \frac{1}{L_j^1}\right)^2} \ge \frac{\left(\frac{1}{p}\sum_{i=1}^p \frac{L_i^0}{L_i^1}\right)\left(\frac{1}{p}\sum_{i=1}^p \frac{1}{L_i^1}\right)}{\frac{1}{p}\left(\frac{1}{p}\sum_{j=1}^p \frac{1}{L_j^1}\right)^2} \ge \frac{\left(\frac{1}{p}\sum_{i=1}^p L_i^0\right)\left(\frac{1}{p}\sum_{i=1}^p \frac{1}{L_i^1}\right)}{\frac{1}{p}\left(\frac{1}{p}\sum_{j=1}^p \frac{1}{L_j^1}\right)} = \sum_{i=1}^p L_i^0.$$

Conversely, if both sequences $\{L_i^0\}$ and $\{L_i^1\}$ are sorted in the same order (either increasing or decreasing), the inequality reverses, and the first term of (18) may be tighter. That said, empirical evidence we provide in Section 5 indicates that in practice $L_i^0 \approx 0$ across all layers, in which case the first terms in (16) and (18) effectively vanish. Then, (18) is clearly superior, replacing the worst-case constant $L_{\max}^1$ by the harmonic mean.

Proof. We start with the result obtained in Lemma 1 with $X = X^k$ and $Y = X^{k+1}$

$$\begin{aligned} f(X^{k+1}) &\le f(X^k) + \left\langle \nabla f(X^k), X^{k+1} - X^k \right\rangle + \sum_{i=1}^p \frac{L_i^0 + L_i^1 \|\nabla_i f(X^k)\|_{(i)\star}}{2} \|X_i^k - X_i^{k+1}\|_{(i)}^2 \\ &= f(X^k) + \sum_{i=1}^p \left[\left\langle \nabla_i f(X^k), X_i^{k+1} - X_i^k \right\rangle_{(i)} + \frac{L_i^0 + L_i^1 \|\nabla_i f(X^k)\|_{(i)\star}}{2} \|X_i^k - X_i^{k+1}\|_{(i)}^2 \right]. \end{aligned}$$

The update rule (12) and the definition of the dual norm $\|\cdot\|_{(i)\star}$ give

$$\|X_i^k - X_i^{k+1}\|_{(i)}^2 \le \left(t_i^k\right)^2$$

and

$$\begin{aligned} \left\langle \nabla_i f(X^k), X_i^{k+1} - X_i^k \right\rangle_{(i)} &= \left\langle \nabla_i f(X^k), \mathrm{LMO}_{\mathcal{B}_i^k}\left(\nabla_i f(X^k)\right) - X_i^k \right\rangle_{(i)} \\ &= -t_i^k \max_{\|X_i\|_{(i)} \le 1} \left\langle \nabla_i f(X^k), X_i \right\rangle_{(i)} \\ &= -t_i^k \|\nabla_i f(X^k)\|_{(i)\star}. \end{aligned}$$

Consequently,

$$f(X^{k+1}) \le f(X^k) + \sum_{i=1}^p \left[-t_i^k \|\nabla_i f(X^k)\|_{(i)\star} + \frac{L_i^0 + L_i^1 \|\nabla_i f(X^k)\|_{(i)\star}}{2} \left(t_i^k\right)^2 \right].$$

Now, choosing

$$t_i^k = \frac{\|\nabla_i f(X^k)\|_{(i)\star}}{L_i^0 + L_i^1 \|\nabla_i f(X^k)\|_{(i)\star}},$$

which minimizes the right-hand side of the last inequality, yields the descent inequality

$$f(X^{k+1}) \leq f(X^k) - \sum_{i=1}^{p} \frac{\|\nabla_i f(X^k)\|_{(i)\star}^2}{2\left(L_i^0 + L_i^1 \|\nabla_i f(X^k)\|_{(i)\star}\right)}. \tag{19}$$

Summing the terms, we obtain

$$\begin{aligned} \sum_{k=0}^{K-1} \sum_{i=1}^{p} \frac{\|\nabla_i f(X^k)\|_{(i)\star}^2}{2\left(L_i^0 + L_i^1 \|\nabla_i f(X^k)\|_{(i)\star}\right)} &\leq \sum_{k=0}^{K-1} \left(f(X^k) - f(X^{k+1})\right) \\ &= f(X^0) - f(X^K) \\ &\leq f(X^0) - \inf_{X \in \mathcal{S}} f(X) =: \Delta^0. \end{aligned} \tag{20}$$

Now, the analysis can proceed in two ways:

1. Upper-bounding L_i^1 by $L_{\max}^1 := \max_{i=1,\ldots,p} L_i^1$ in (20), we obtain

$$\sum_{k=0}^{K-1} \sum_{i=1}^{p} \frac{\|\nabla_i f(X^k)\|_{(i)\star}^2}{2\left(L_i^0 + L_{\max}^1 \|\nabla_i f(X^k)\|_{(i)\star}\right)} \leq \Delta^0. \tag{21}$$

   Now, applying Lemma 3 with $x_i = 1$, $y_i = \|\nabla_i f(X^k)\|_{(i)\star}$ and $z_i = 2\left(L_i^0 + L_{\max}^1 \left\|\nabla_i f(X^k)\right\|_{(i)\star}\right)$ gives

$$\begin{aligned} \phi\left(\sum_{i=1}^{p} \|\nabla_i f(X^k)\|_{(i)\star}\right) &= \frac{\left(\sum_{i=1}^{p} \|\nabla_i f(X^k)\|_{(i)\star}\right)^2}{2\left(\sum_{i=1}^{p} L_i^0 + L_{\max}^1 \sum_{i=1}^{p} \|\nabla_i f(X^k)\|_{(i)\star}\right)} \\ &\leq \sum_{i=1}^{p} \frac{\|\nabla_i f(X^k)\|_{(i)\star}^2}{2\left(L_i^0 + L_{\max}^1 \|\nabla_i f(X^k)\|_{(i)\star}\right)}, \end{aligned}$$

   where $\phi(t) := \frac{t^2}{2(\sum_{i=1}^{p} L_i^0 + L_{\max}^1 t)}$. Combining the last inequality with (21) and using the fact that ϕ is increasing, we obtain

$$K\phi\left(\min_{k=0,\ldots,K-1} \sum_{i=1}^{p} \|\nabla_i f(X^k)\|_{(i)\star}\right) \leq \sum_{k=0}^{K-1} \phi\left(\sum_{i=1}^{p} \|\nabla_i f(X^k)\|_{(i)\star}\right) \leq \Delta^0, \tag{22}$$

   and hence

$$\min_{k=0,\ldots,K-1} \sum_{i=1}^{p} \|\nabla_i f(X^k)\|_{(i)\star} \leq \phi^{-1}\left(\frac{\Delta^0}{K}\right),$$

   where ϕ^{-1} is the inverse function (which exists since ϕ is increasing). Therefore, to reach the precision $\min_{k=0,\ldots,K-1} \sum_{i=1}^{p} \left\|\nabla_i f(X^k)\right\|_{(i)\star} \leq \epsilon$, it is sufficient to choose the number of iterations to be

$$K = \left\lceil \frac{\Delta^0}{\phi(\epsilon)} \right\rceil = \left\lceil \frac{2\sum_{i=1}^{p} L_i^0 \Delta^0}{\epsilon^2} + \frac{2L_{\max}^1 \Delta^0}{\epsilon} \right\rceil.$$

2. Alternatively, we can start from the inequality (20) and apply Lemma 3 with $x_i = 1/L_i^1$, $y_i = \left\|\nabla_i f(X^k)\right\|_{(i)\star}$ and $z_i = 2(L_i^0 + L_i^1 \left\|\nabla_i f(X^k)\right\|_{(i)\star})$ to obtain

$$\begin{aligned} \Delta^0 &\geq \sum_{k=0}^{K-1} \sum_{i=1}^{p} \frac{\|\nabla_i f(X^k)\|_{(i)\star}^2}{2\left(L_i^0 + L_i^1 \|\nabla_i f(X^k)\|_{(i)\star}\right)} \\ &\geq \sum_{k=0}^{K-1} \frac{\left(\sum_{i=1}^{p} \frac{1}{L_i^1} \left\|\nabla_i f(X^k)\right\|_{(i)\star}\right)^2}{2\left(\sum_{i=1}^{p} \frac{1}{(L_i^1)^2} \left(L_i^0 + L_i^1 \left\|\nabla_i f(X^k)\right\|_{(i)\star}\right)\right)} \end{aligned}$$

$$= \sum_{k=0}^{K-1} \frac{\left(\sum_{i=1}^p \frac{1}{L_i^1} \left\|\nabla_i f(X^k)\right\|_{(i)\star}\right)^2}{2\left(\sum_{i=1}^p \frac{L_i^0}{(L_i^1)^2} + \sum_{i=1}^p \frac{1}{L_i^1} \left\|\nabla_i f(X^k)\right\|_{(i)\star}\right)}$$
$$= \sum_{t=0}^{K-1} \psi\left(\sum_{i=1}^p \frac{1}{L_i^1} \left\|\nabla_i f(X^k)\right\|_{(i)\star}\right),$$

where $\psi(t) := \frac{t^2}{2\left(\sum_{i=1}^p \frac{L_i^0}{(L_i^1)^2} + t\right)}$. Since the function ψ is increasing for $t > 0$, ψ^{-1} exists. It follows that

$$\Delta^0 \geq \sum_{k=0}^{K-1} \psi\left(\sum_{i=1}^p \frac{1}{L_i^1} \left\|\nabla_i f(X^k)\right\|_{(i)\star}\right)$$
$$\geq K\psi\left(\min_{k=0,\ldots,K-1} \sum_{i=1}^p \frac{1}{L_i^1} \left\|\nabla_i f(X^k)\right\|_{(i)\star}\right),$$

and hence

$$\min_{k=0,\ldots,K-1} \sum_{i=1}^p \frac{1}{L_i^1} \left\|\nabla_i f(X^k)\right\|_{(i)\star} \leq \psi^{-1}\left(\frac{\Delta^0}{K}\right).$$

This in turn means that to reach the precision

$$\min_{k=0,\ldots,K-1} \sum_{i=1}^p \left[\frac{\frac{1}{L_i^1}}{\frac{1}{p}\sum_{j=1}^p \frac{1}{L_j^1}} \left\|\nabla_i f(X^k)\right\|_{(i)\star}\right] \leq \varepsilon,$$

it suffices to run the algorithm for

$$K = \left\lceil \frac{\Delta^0}{\psi\left(\varepsilon\left(\frac{1}{p}\sum_{j=1}^p \frac{1}{L_j^1}\right)\right)} \right\rceil = \left\lceil \frac{2\Delta^0\left(\sum_{i=1}^p \frac{L_i^0}{(L_i^1)^2}\right)}{\varepsilon^2\left(\frac{1}{p}\sum_{j=1}^p \frac{1}{L_j^1}\right)^2} + \frac{2\Delta^0}{\varepsilon\left(\frac{1}{p}\sum_{j=1}^p \frac{1}{L_j^1}\right)} \right\rceil$$

iterations.

□

D.3 Convergence under the PŁ condition

We now establish convergence rates under the layer-wise Polyak–Łojasiewicz (PŁ) condition, introduced in Assumption 3. This property is especially relevant for heavily over-parameterized neural networks, as it has been shown to capture the properties of their loss landscapes (Liu et al., 2022).

Assumption 3 (Layer-wise Polyak-Łojasiewicz condition)**.** *The function $f : \mathcal{S} \mapsto \mathbb{R}$ satisfies the layer-wise Polyak-Łojasiewicz (PŁ) condition with a constant $\mu > 0$, i.e., for any $X \in \mathcal{S}$*

$$\sum_{i=1}^p \|\nabla_i f(X)\|_{(i)\star}^2 \geq 2\mu\left(f(X) - f^\star\right),$$

where $f^\star := \inf_{X\in\mathcal{S}} f(X) > -\infty$.

Assumption 3 reduces to the standard PŁ condition (Karimi et al., 2020) by vectorizing the parameters and adopting the Euclidean norm $\|\cdot\|_2$.

Theorem 5. *Let Assumptions 1 and 3 hold and fix $\varepsilon > 0$. Let $X^0, \ldots, X^{K-1}$ be the iterates of deterministic Gluon (Algorithm 2) run with $t_i^k = \frac{\|\nabla_i f(X^k)\|_{(i)\star}}{L_i^0 + L_i^1 \|\nabla_i f(X^k)\|_{(i)\star}}$.*

1. *If $L_i^1 \geq 0$, then to reach the precision $\min_{k=0,\ldots,K-1} f(X^k) - f^\star \leq \epsilon$, it suffices to run the algorithm for*

$$K = \left\lceil \frac{\sum_{i=1}^p L_i^0 \Delta^0}{\mu\epsilon} + \frac{\sqrt{2}L_{\max}^1 \Delta^0}{\sqrt{\mu\epsilon}} \right\rceil$$

iterations,

2. *If $L_i^1 = 0$ for all $i = 1, \ldots, p$, then to reach the precision $f(X^K) - f^\star \leq \epsilon$, it suffices to run the algorithm for*

$$K = \left\lceil \frac{L_{\max}^0}{\mu} \log \frac{\Delta^0}{\epsilon} \right\rceil,$$

where $L_{\max}^0 := \max_{i=1,\ldots,p} L_i^0$, $L_{\max}^1 := \max_{i=1,\ldots,p} L_i^1$, $\Delta^0 := f(X^0) - f^\star$ *and* $f^\star := \inf_{X \in \mathcal{S}} f(X)$.

Proof. We consider two scenarios: (1) the general case with arbitrary $L_i^1 \geq 0$ and (2) $L_i^1 = 0$ for all $i = 1, \ldots, p$.

Case 1: $L_i^1 \geq 0$**.** We start by following the same steps as in the proof of Theorem 1. From (22), we have

$$\sum_{k=0}^{K-1} \phi\left(\sum_{i=1}^p \|\nabla_i f(X^k)\|_{(i)\star}\right) \leq \Delta^0,$$

where $\phi(t) := \frac{t^2}{2(\sum_{i=1}^p L_i^0 + L_{\max}^1 t)}$. Now, using Assumption 3, we get

$$\left(\sum_{i=1}^p \|\nabla_i f(X^k)\|_{(i)\star}\right)^2 \geq \sum_{i=1}^p \|\nabla_i f(X^k)\|_{(i)\star}^2 \geq 2\mu \left(f(X^k) - f^\star\right).$$

Consequently, since ϕ is an increasing function,

$$\begin{aligned} K\phi\left(\sqrt{2\mu}\sqrt{f(X^{k^\star}) - f^\star}\right) &\leq \sum_{k=0}^{K-1} \phi\left(\sqrt{2\mu}\sqrt{f(X^k) - f^\star}\right) \\ &\leq \sum_{k=0}^{K-1} \phi\left(\sum_{i=1}^p \|\nabla_i f(X^k)\|_{(i)\star}\right) \leq \Delta^0, \end{aligned}$$

where $k^\star := \operatorname{argmin}_{k=0,\ldots,K-1} f(X^k) - f^\star$. Denoting the corresponding inverse function (which exists since ϕ is increasing) by ϕ^{-1}, it follows that

$$\sqrt{2\mu}\sqrt{f(X^{k^\star}) - f^\star} \leq \phi^{-1}\left(\frac{\Delta^0}{K}\right) \leq \sqrt{2\mu\epsilon}.$$

Therefore, to reach the precision $f(X^{k^\star}) - f^\star \leq \epsilon$, it is sufficient to choose the number of iterations

$$K = \left\lceil \frac{\Delta^0}{\phi\left(\sqrt{2\mu\epsilon}\right)} \right\rceil = \left\lceil \frac{\sum_{i=1}^p L_i^0 \Delta^0}{\mu\epsilon} + \frac{\sqrt{2} L_{\max}^1 \Delta^0}{\sqrt{\mu\epsilon}} \right\rceil.$$

Case 2: $L_i^1 = 0$**.** Inequality (19) from the proof of Theorem 1 with $L_i^1 = 0$ gives

$$f(X^{k+1}) \leq f(X^k) - \sum_{i=1}^p \frac{\|\nabla_i f(X^k)\|_{(i)\star}^2}{2L_i^0}.$$

Using the fact that

$$\sum_{i=1}^p \frac{\|\nabla_i f(X^k)\|_{(i)\star}^2}{2L_i^0} \geq \min_{j=1,\ldots,p} \frac{1}{2L_j^0} \sum_{i=1}^p \|\nabla_i f(X^k)\|_{(i)\star}^2 = \frac{1}{2\max_{j=1,\ldots,p} L_j^0} \sum_{i=1}^p \|\nabla f(X^k)\|_{(i)\star}^2$$

along with Assumption 3, we obtain

$$f(X^{k+1}) \leq f(X^k) - \frac{\mu}{L_{\max}^0}\left(f(X^k) - f^\star\right).$$

The remaining part of the proof follows from the simple observation

$$\log\left(\frac{\Delta_0}{\epsilon}\right) \leq k\frac{\mu}{L_{\max}^0} \leq k \log\left(\frac{1}{1 - \frac{\mu}{L_{\max}^0}}\right).$$

□

E STOCHASTIC CASE

E.1 ADAPTIVE STEPSIZES

Before proving the main result from Section 4.3, we first present an attempt to formulate an adaptive stepsize strategy for the stochastic setting. This requires the following assumption:

Assumption 4. *The stochastic gradient estimator $\nabla f_\xi : \mathcal{S} \mapsto \mathcal{S}$ is unbiased and has bounded relative variance. That is, $\mathbb{E}[\nabla f_\xi(X)] = \nabla f(X)$ for all $X \in \mathcal{S}$ and there exists $0 \leq \zeta < 1$ such that*

$$\|\nabla_i f_\xi(X) - \nabla_i f(X)\|_{(i)\star} \leq \zeta \|\nabla_i f_\xi(X)\|_{(i)\star}, \qquad i = 1, \ldots, p$$

holds almost surely for all $X \in \mathcal{S}$.

This assumption is somewhat unconventional due to the presence of the stochastic gradients on the right-hand side of the inequality. It does not follow from standard conditions and does not fall within known frameworks for modeling stochasticity, such as the ABC inequality of Khaled & Richtárik (2020). Instead, it introduces a novel structure with parallels to the literature on contractive compression (Beznosikov et al., 2023; Demidovich et al., 2023).

To elaborate, recall the definition of a contractive compressor:

Definition 6 (Contractive compressor)**.** A stochastic mapping $\mathcal{C} : \mathcal{S} \to \mathcal{S}$ is called a *contractive compressor* if there exists $\alpha \in [0, 1)$ such that

$$\mathbb{E}\left[\|\mathcal{C}(X) - X\|^2\right] \leq (1 - \alpha)\|X\|^2 \tag{23}$$

for any $X \in \mathcal{S}$.

There is a conceptual similarity between Assumption 4 and the contractive property in (23). Assumption 4 can be interpreted as asserting that the true gradient $\nabla f(X)$ is effectively a contraction of the stochastic gradient $\nabla f_\xi(X)$, with contraction factor $1 - \zeta$. Unlike contractive compressors, there is no explicit mapping from $\nabla f_\xi(X)$ to $\nabla f(X)$, and the uniform bound implies the same contraction-like behavior across all stochastic gradients.

Although Assumption 4 is admittedly strong, it allows us to establish a convergence theorem using an adaptive stepsize strategy similar to the one employed in the deterministic case in Theorem 3.

Theorem 7. *Let Assumptions 1 and 4 hold and fix $\varepsilon > 0$. Let $X^0, \ldots, X^{K-1}$ be the iterates of* Gluon *(Algorithm 1) run with $\beta^k = 0$ and $t_i^k = \frac{(1-\zeta)\|\nabla_i f_{\xi^k}(X^k)\|_{(i)\star}}{L_i^0 + (1+\zeta)L_i^1 \|\nabla_i f_{\xi^k}(X^k)\|_{(i)\star}}$. Then,*

1. *In order to reach the precision*

$$\min_{k=0,\ldots,K-1} \sum_{i=1}^p \mathbb{E}\left[\left\|\nabla_i f(X^k)\right\|_{(i)\star}\right] \leq \epsilon,$$

it suffices to run the algorithm for

$$K = \left\lceil \frac{2\sum_{i=1}^p L_i^0 \Delta^0}{(1-\zeta)^2 \epsilon^2} + \frac{2(1+\zeta)L_{\max}^1 \Delta^0}{(1-\zeta)^2 \epsilon} \right\rceil$$

iterations.

2. *In order to reach the precision*

$$\min_{k=0,\ldots,K-1} \sum_{i=1}^p \left[\frac{\frac{1}{L_i^1}}{\frac{1}{p}\sum_{j=1}^p \frac{1}{L_j^1}} \left\|\nabla_i f(X^k)\right\|_{(i)\star} \right] \leq \varepsilon,$$

it suffices to run the algorithm for

$$K = \left\lceil \frac{2\Delta^0 \sum_{i=1}^p \frac{L_i^0}{(L_i^1)^2}}{\varepsilon^2(1-\zeta)^2 \left(\frac{1}{p}\sum_{j=1}^p \frac{1}{L_j^1}\right)^2} + \frac{2\Delta^0(1+\zeta)}{\varepsilon(1-\zeta)^2 \left(\frac{1}{p}\sum_{j=1}^p \frac{1}{L_j^1}\right)} \right\rceil$$

iterations,

where $\Delta^0 := f(X^0) - \inf_{X \in \mathcal{S}} f(X)$ and $L_{\max}^1 := \max_{i=1,\ldots,p} L_i^1$.

Proof. Lemma 1 with $X = X^k$ and $Y = X^{k+1}$ gives

$$\begin{aligned}
& f(X^{k+1}) \\
\leq\ & f(X^k) + \left\langle \nabla f(X^k), X^{k+1} - X^k \right\rangle + \sum_{i=1}^{p} \frac{L_i^0 + L_i^1 \|\nabla_i f(X^k)\|_{(i)\star}}{2} \|X_i^k - X_i^{k+1}\|_{(i)}^2 \\
=\ & f(X^k) + \sum_{i=1}^{p} \left[\left\langle \nabla_i f(X^k), X_i^{k+1} - X_i^k \right\rangle_{(i)} + \frac{L_i^0 + L_i^1 \|\nabla_i f(X^k)\|_{(i)\star}}{2} \|X_i^k - X_i^{k+1}\|_{(i)}^2 \right] \\
=\ & f(X^k) + \sum_{i=1}^{p} \left[\left\langle \nabla_i f_{\xi^k}(X^k), X_i^{k+1} - X_i^k \right\rangle_{(i)} + \left\langle \nabla_i f(X^k) - \nabla_i f_{\xi^k}(X^k), X_i^{k+1} - X_i^k \right\rangle_{(i)} \right] \\
& + \sum_{i=1}^{p} \frac{L_i^0 + L_i^1 \|\nabla_i f(X^k)\|_{(i)\star}}{2} \|X_i^k - X_i^{k+1}\|_{(i)}^2,
\end{aligned}$$

and applying the Cauchy-Schwarz inequality, we get

$$\begin{aligned}
f(X^{k+1}) \leq f(X^k) + \sum_{i=1}^{p} \Bigg[& \left\langle \nabla_i f_{\xi^k}(X^k), X_i^{k+1} - X_i^k \right\rangle_{(i)} \\
& + \|\nabla_i f(X^k) - \nabla_i f_{\xi^k}(X^k)\|_{(i)\star} \|X_i^{k+1} - X_i^k\|_{(i)} \\
& + \frac{L_i^0 + L_i^1 \|\nabla_i f(X^k)\|_{(i)\star}}{2} \|X_i^k - X_i^{k+1}\|_{(i)}^2 \Bigg].
\end{aligned}$$

The update rule (1) and the definition of the dual norm $\|\cdot\|_{(i)\star}$ give

$$\|X_i^k - X_i^{k+1}\|_{(i)}^2 \leq \left(t_i^k\right)^2$$

and

$$\begin{aligned}
\left\langle \nabla_i f_{\xi^k}(X^k), X_i^{k+1} - X_i^k \right\rangle_{(i)} &= \left\langle \nabla_i f_{\xi^k}(X^k), \mathrm{LMO}_{\mathcal{B}_i^k}\left(\nabla_i f_{\xi^k}(X^k)\right) - X_i^k \right\rangle_{(i)} \\
&= -t_i^k \max_{\|X_i\|_{(i)} \leq 1} \left\langle \nabla_i f_{\xi^k}(X^k), X_i \right\rangle_{(i)} \\
&= -t_i^k \|\nabla_i f_{\xi^k}(X^k)\|_{(i)\star}.
\end{aligned}$$

Consequently, using Assumption 4, we obtain

$$\begin{aligned}
f(X^{k+1}) &\leq f(X^k) + \sum_{i=1}^{p} \Bigg[- t_i^k \|\nabla_i f_{\xi^k}(X^k)\|_{(i)\star} + t_i^k \|\nabla_i f(X^k) - \nabla_i f_{\xi^k}(X^k)\|_{(i)\star} \\
&\qquad + \frac{L_i^0 + L_i^1 \|\nabla_i f(X^k)\|_{(i)\star}}{2} \left(t_i^k\right)^2 \Bigg] \\
&\leq f(X^k) + \sum_{i=1}^{p} \Bigg[- (1-\zeta) t_i^k \|\nabla_i f_{\xi^k}(X^k)\|_{(i)\star} \\
&\qquad + \frac{L_i^0 + (1+\zeta) L_i^1 \|\nabla_i f_{\xi^k}(X^k)\|_{(i)\star}}{2} \left(t_i^k\right)^2 \Bigg].
\end{aligned}$$

Minimizing the right-hand side of the last inequality with respect to t_i^k yields

$$t_i^k = \frac{(1-\zeta)\|\nabla_i f_{\xi^k}(X^k)\|_{(i)\star}}{L_i^0 + (1+\zeta) L_i^1 \|\nabla_i f_{\xi^k}(X^k)\|_{(i)\star}}.$$

This greedy approach for choosing t_i^k gives the descent inequality

$$f(X^{k+1}) \leq f(X^k) - \sum_{i=1}^{p} \frac{(1-\zeta)^2 \|\nabla_i f_{\xi^k}(X^k)\|_{(i)\star}^2}{2\left(L_i^0 + (1+\zeta) L_i^1 \|\nabla_i f_{\xi^k}(X^k)\|_{(i)\star}\right)}.$$

Taking expectations, we have

$$\mathbb{E}[f(X^{k+1})] \leq \mathbb{E}[f(X^k)] - \sum_{i=1}^{p} \mathbb{E}\left[\frac{(1-\zeta)^2 \|\nabla_i f_{\xi^k}(X^k)\|^2_{(i)\star}}{2\left(L_i^0 + (1+\zeta)L_i^1 \|\nabla_i f_{\xi^k}(X^k)\|_{(i)\star}\right)}\right]. \tag{24}$$

Now, let us define the function $\phi_i(t) := \frac{(1-\zeta)^2 t^2}{2(L_i^0 + (1+\zeta)L_i^1 t)}$. Since $\phi_i(t)$ is convex, Jensen's inequality gives

$$\begin{aligned}\mathbb{E}[f(X^k)] - \mathbb{E}[f(X^{k+1})] &\geq \sum_{i=1}^{p} \mathbb{E}\left[\frac{(1-\zeta)^2 \|\nabla_i f_{\xi^k}(X^k)\|^2_{(i)\star}}{2\left(L_i^0 + (1+\zeta)L_i^1 \|\nabla_i f_{\xi^k}(X^k)\|_{(i)\star}\right)}\right] \\ &\geq \sum_{i=1}^{p} \frac{(1-\zeta)^2 \left(\mathbb{E}\left[\|\nabla_i f_{\xi^k}(X^k)\|_{(i)\star}\right]\right)^2}{2\left(L_i^0 + (1+\zeta)L_i^1 \mathbb{E}\left[\|\nabla_i f_{\xi^k}(X^k)\|_{(i)\star}\right]\right)}.\end{aligned}$$

By Jensen's inequality and Assumption 4

$$\begin{aligned}\mathbb{E}\left[\left\|\nabla_i f(X^k)\right\|_{(i)\star}\right] &= \mathbb{E}\left[\left\|\mathbb{E}\left[\nabla_i f_{\xi_k}(X^k)\middle| X^k\right]\right\|_{(i)\star}\right] \\ &\leq \mathbb{E}\left[\mathbb{E}\left[\left\|\nabla_i f_{\xi_k}(X^k)\right\|_{(i)\star}\middle| X^k\right]\right] \\ &= \mathbb{E}\left[\left\|\nabla_i f_{\xi_k}(X^k)\right\|_{(i)\star}\right],\end{aligned}$$

and hence, using the fact that ϕ_i is increasing, we get

$$\mathbb{E}[f(X^k)] - \mathbb{E}[f(X^{k+1})] \geq \sum_{i=1}^{p} \frac{(1-\zeta)^2 \left(\mathbb{E}\left[\left\|\nabla_i f(X^k)\right\|_{(i)\star}\right]\right)^2}{2\left(L_i^0 + (1+\zeta)L_i^1 \mathbb{E}\left[\|\nabla_i f(X^k)\|_{(i)\star}\right]\right)}.$$

Summing the terms gives

$$\begin{aligned}\sum_{k=0}^{K-1}\sum_{i=1}^{p} \frac{(1-\zeta)^2 \left(\mathbb{E}\left[\left\|\nabla_i f(X^k)\right\|_{(i)\star}\right]\right)^2}{2\left(L_i^0 + (1+\zeta)L_i^1 \mathbb{E}\left[\|\nabla_i f(X^k)\|_{(i)\star}\right]\right)} &\leq \sum_{k=0}^{K-1} \left(\mathbb{E}[f(X^k)] - \mathbb{E}[f(X^{k+1})]\right) \\ &= \mathbb{E}[f(X^0)] - \mathbb{E}[f(X^K)] \\ &\leq f(X^0) - \inf_{X\in\mathcal{S}} f(X) =: \Delta^0,\end{aligned} \tag{25}$$

The remaining part of the proof closely follows the proof of Theorem 3. We can proceed in two ways:

1. Upper-bounding L_i^1 by $L_{\max}^1 := \max_{i=1,\ldots,p} L_i^1$ in (25), we obtain

$$\sum_{k=0}^{K-1}\sum_{i=1}^{p} \frac{(1-\zeta)^2 \left(\mathbb{E}\left[\left\|\nabla_i f(X^k)\right\|_{(i)\star}\right]\right)^2}{2\left(L_i^0 + (1+\zeta)L_{\max}^1 \mathbb{E}\left[\|\nabla_i f(X^k)\|_{(i)\star}\right]\right)} \leq \Delta^0. \tag{26}$$

   Now, Lemma 3 with $x_i = 1$, $y_i = (1-\zeta)\mathbb{E}\left[\|\nabla_i f(X^k)\|_{(i)\star}\right]$ and $z_i = 2\left(L_i^0 + (1+\zeta)L_{\max}^1 \mathbb{E}\left[\left\|\nabla_i f(X^k)\right\|_{(i)\star}\right]\right)$ gives

$$\begin{aligned}\phi\left(\sum_{i=1}^{p} \mathbb{E}\left[\|\nabla_i f(X^k)\|_{(i)\star}\right]\right) &= \frac{\left((1-\zeta)\sum_{i=1}^{p} \mathbb{E}\left[\|\nabla_i f(X^k)\|_{(i)\star}\right]\right)^2}{2\sum_{i=1}^{p}\left(L_i^0 + (1+\zeta)L_{\max}^1 \mathbb{E}\left[\|\nabla_i f(X^k)\|_{(i)\star}\right]\right)} \\ &\leq \sum_{i=1}^{p} \frac{(1-\zeta)^2 \mathbb{E}\left[\|\nabla_i f(X^k)\|_{(i)\star}\right]^2}{2\left(L_i^0 + (1+\zeta)L_{\max}^1 \mathbb{E}\left[\|\nabla_i f(X^k)\|_{(i)\star}\right]\right)}\end{aligned}$$

   where $\phi(t) := \frac{(1-\zeta)^2 t^2}{2(\sum_{i=1}^p L_i^0 + (1+\zeta)L_{\max}^1 t)}$. Combining the last inequality with (26) and using the fact that ϕ is increasing, we get

$$K\phi\left(\min_{k=0,\ldots,K-1} \sum_{i=1}^{p} \mathbb{E}\left[\|\nabla_i f(X^k)\|_{(i)\star}\right]\right) \leq \sum_{k=0}^{K-1} \phi\left(\sum_{i=1}^{p} \mathbb{E}\left[\|\nabla_i f(X^k)\|_{(i)\star}\right]\right) \leq \Delta^0.$$

and hence

$$\min_{k=0,\ldots,K-1} \sum_{i=1}^{p} \mathbb{E}\left[\|\nabla_i f(X^k)\|_{(i)\star}\right] \leq \phi^{-1}\left(\frac{\Delta^0}{K}\right),$$

where ϕ^{-1} denotes the inverse function (which exists since ϕ is increasing). Therefore, to reach the precision $\min_{k=0,\ldots,K-1} \sum_{i=1}^{p} \mathbb{E}\left[\|\nabla_i f(X^k)\|_{(i)\star}\right] \leq \epsilon$, it suffices to run the algorithm for

$$K = \left\lceil \frac{\Delta^0}{\phi(\epsilon)} \right\rceil = \left\lceil \frac{2\Delta^0 \sum_{i=1}^{p} L_i^0}{(1-\zeta)^2\epsilon^2} + \frac{2\Delta^0(1+\zeta)L_{\max}^1}{(1-\zeta)^2\epsilon} \right\rceil$$

iterations.

2. Alternatively, we can start from inequality (25) and apply Lemma 3 with $x_i = {}^1/_{L_i^1}$, $y_i = (1-\zeta)\mathbb{E}\left[\left\|\nabla_i f(X^k)\right\|_{(i)\star}\right]$ and $z_i = 2\left(L_i^0 + (1+\zeta)L_i^1\mathbb{E}\left[\left\|\nabla_i f(X^k)\right\|_{(i)\star}\right]\right)$ to obtain

$$\begin{aligned}
\Delta^0 &\geq \sum_{k=0}^{K-1}\sum_{i=1}^{p} \frac{(1-\zeta)^2\mathbb{E}\left[\left\|\nabla_i f(X^k)\right\|_{(i)\star}\right]^2}{2\left(L_i^0 + (1+\zeta)L_i^1\mathbb{E}\left[\|\nabla_i f(X^k)\|_{(i)\star}\right]\right)} \\
&\geq \sum_{k=0}^{K-1} \frac{\left(\sum_{i=1}^{p} \frac{1}{L_i^1}(1-\zeta)\mathbb{E}\left[\left\|\nabla_i f(X^k)\right\|_{(i)\star}\right]\right)^2}{2\sum_{i=1}^{p}\left(\frac{L_i^0}{(L_i^1)^2} + (1+\zeta)\frac{1}{L_i^1}\mathbb{E}\left[\|\nabla_i f(X^k)\|_{(i)\star}\right]\right)} \\
&= \sum_{t=0}^{K-1} \psi\left(\sum_{i=1}^{p} \frac{1}{L_i^1}\mathbb{E}\left[\left\|\nabla_i f(X^k)\right\|_{(i)\star}\right]\right),
\end{aligned}$$

where $\psi(t) := \frac{(1-\zeta)^2 t^2}{2\left(\sum_{i=1}^{p} \frac{L_i^0}{(L_i^1)^2} + (1+\zeta)t\right)}$. Since the function ψ is increasing for $t > 0$, ψ^{-1} exists. It follows that

$$\begin{aligned}
\Delta^0 &\geq \sum_{k=0}^{K-1} \psi\left(\sum_{i=1}^{p} \frac{1}{L_i^1}\mathbb{E}\left[\left\|\nabla_i f(X^k)\right\|_{(i)\star}\right]\right) \\
&\geq K\psi\left(\min_{k=0,\ldots,K-1} \sum_{i=1}^{p} \frac{1}{L_i^1}\mathbb{E}\left[\left\|\nabla_i f(X^k)\right\|_{(i)\star}\right]\right),
\end{aligned}$$

and hence

$$\min_{k=0,\ldots,K-1} \sum_{i=1}^{p} \frac{1}{L_i^1}\mathbb{E}\left[\left\|\nabla_i f(X^k)\right\|_{(i)\star}\right] \leq \psi^{-1}\left(\frac{\Delta^0}{K}\right).$$

This in turn means that to reach the precision

$$\min_{k=0,\ldots,K-1} \sum_{i=1}^{p} \left[\frac{\frac{1}{L_i^1}}{\frac{1}{p}\sum_{j=1}^{p}\frac{1}{L_j^1}}\left\|\nabla_i f(X^k)\right\|_{(i)\star}\right] \leq \varepsilon,$$

it suffices to run the algorithm for

$$\begin{aligned}
K &= \left\lceil \frac{\Delta^0}{\psi\left(\varepsilon\left(\frac{1}{p}\sum_{j=1}^{p}\frac{1}{L_j^1}\right)\right)} \right\rceil \\
&= \left\lceil \frac{2\Delta^0\sum_{i=1}^{p}\frac{L_i^0}{(L_i^1)^2}}{(1-\zeta)^2\varepsilon^2\left(\frac{1}{p}\sum_{j=1}^{p}\frac{1}{L_j^1}\right)^2} + \frac{2\Delta^0(1+\zeta)}{(1-\zeta)^2\varepsilon\left(\frac{1}{p}\sum_{j=1}^{p}\frac{1}{L_j^1}\right)} \right\rceil
\end{aligned}$$

iterations.

□

E.2 Proof of Theorem 2

We now establish the main result of Section 4.3. The guarantees in Theorem 2 follow from the more general result below. Here, $\rho_i > 0$ for $i \in [p]$ denote the norm equivalence constants, i.e., $\|X_i\|_{(i)\star} \leq \rho_i \|X_i\|_2$ for all $X_i \in \mathcal{S}_i$.

Theorem 8. *Let Assumptions 1 and 2 hold and fix $\varepsilon > 0$. Let $X^0, \ldots, X^{K-1}$ be the iterates of* Gluon *(Algorithm 1) run with $\beta^k = 1 - (k+1)^{-1/2}$, $t_i^k = t_i(k+1)^{-3/4}$ for some $t_i > 0$, and $M_i^0 = \nabla_i f_{\xi^0}(X^0)$.*

1. *If $L_i^1 = 0$, then*

$$\min_{k=0,\ldots,K-1} \sum_{i=1}^p t_i \mathbb{E}\left[\|\nabla_i f(X^k)\|_{(i)\star}\right] \leq \frac{\Delta^0}{K^{1/4}} + \frac{1}{K^{1/4}} \sum_{i=1}^p \left[\sigma\rho_i t_i \left(7 + 2\sqrt{2e^2}\log(K)\right) + L_i^0 t_i^2 \left(\frac{87}{2} + 14\log(K)\right)\right],$$

2. *If $L_i^1 \neq 0$, then for $t_i = \frac{1}{12L_i^1}$, we have*

$$\min_{k=0,\ldots,K-1} \sum_{i=1}^p \frac{1}{12L_i^1} \mathbb{E}\left[\|\nabla_i f(X^k)\|_{(i)\star}\right] \leq \frac{2\Delta^0}{K^{1/4}} + \frac{1}{K^{1/4}} \sum_{i=1}^p \left[\frac{\sigma\rho_i}{6L_i^1}\left(7 + 2\sqrt{2e^2}\log(K)\right) + \frac{L_i^0}{144(L_i^1)^2}\left(87 + 28\log(K)\right)\right],$$

where $\Delta^0 := f(X^0) - \inf_{X\in\mathcal{S}} f(X)$.

Proof. We again start with the result in Lemma 1 with $X = X^k$ and $Y = X^{k+1}$, obtaining

$$\begin{aligned} f(X^{k+1}) &\leq f(X^k) + \left\langle \nabla f(X^k), X^{k+1} - X^k\right\rangle + \sum_{i=1}^p \frac{L_i^0 + L_i^1\|\nabla_i f(X^k)\|_{(i)\star}}{2}\|X_i^k - X_i^{k+1}\|_{(i)}^2 \\ &= f(X^k) + \sum_{i=1}^p \left[\left\langle \nabla_i f(X^k), X_i^{k+1} - X_i^k\right\rangle_{(i)} + \frac{L_i^0 + L_i^1\|\nabla_i f(X^k)\|_{(i)\star}}{2}\|X_i^k - X_i^{k+1}\|_{(i)}^2\right] \\ &= f(X^k) + \sum_{i=1}^p \left[\left\langle M_i^k, X_i^{k+1} - X_i^k\right\rangle_{(i)} + \left\langle \nabla_i f(X^k) - M_i^k, X_i^{k+1} - X_i^k\right\rangle_{(i)}\right] \\ &\quad + \sum_{i=1}^p \frac{L_i^0 + L_i^1\|\nabla_i f(X^k)\|_{(i)\star}}{2}\|X_i^k - X_i^{k+1}\|_{(i)}^2. \end{aligned}$$

Applying the Cauchy-Schwarz inequality, we have

$$\begin{aligned} f(X^{k+1}) &\leq f(X^k) + \sum_{i=1}^p \left[\left\langle M_i^k, X_i^{k+1} - X_i^k\right\rangle_{(i)} + \|\nabla_i f(X^k) - M_i^k\|_{(i)\star}\|X_i^{k+1} - X_i^k\|_{(i)}\right] \\ &\quad + \sum_{i=1}^p \frac{L_i^0 + L_i^1\|\nabla_i f(X^k)\|_{(i)\star}}{2}\|X_i^k - X_i^{k+1}\|_{(i)}^2. \end{aligned}$$

Now, the update rule (1) and the definition of the dual norm $\|\cdot\|_{(i)\star}$ give

$$\|X_i^k - X_i^{k+1}\|_{(i)}^2 \leq \left(t_i^k\right)^2$$

and

$$\left\langle M_i^k, X_i^{k+1} - X_i^k\right\rangle = \left\langle M_i^k, \mathrm{LMO}_{\mathcal{B}_i^k}\left(M_i^k\right) - X_i^k\right\rangle = -t_i^k \max_{\|X_i\|_{(i)}\leq 1} \left\langle M_i^k, X_i\right\rangle = -t_i^k\|M_i^k\|_{(i)\star}.$$

Consequently,

$$
\begin{aligned}
& f(X^{k+1}) \\
\leq\ & f(X^k) + \sum_{i=1}^{p} \left[-t_i^k \|M_i^k\|_{(i)\star} + t_i^k \|\nabla_i f(X^k) - M_i^k\|_{(i)\star} + \frac{L_i^0 + L_i^1 \|\nabla_i f(X^k)\|_{(i)\star}}{2} \left(t_i^k\right)^2 \right] \\
=\ & f(X^k) + \sum_{i=1}^{p} \left[- t_i^k \|M_i^k - \nabla_i f(X^k) + \nabla_i f(X^k)\|_{(i)\star} + t_i^k \|M_i^k - \nabla_i f(X^k)\|_{(i)\star} \right] \\
& + \sum_{i=1}^{p} \frac{L_i^0 + L_i^1 \|\nabla_i f(X^k)\|_{(i)\star}}{2} \left(t_i^k\right)^2 \\
\leq\ & f(X^k) + \sum_{i=1}^{p} \left[-t_i^k \|\nabla_i f(X^k)\|_{(i)\star} + 2t_i^k \|M_i^k - \nabla_i f(X^k)\|_{(i)\star} \right] \\
& + \sum_{i=1}^{p} \frac{L_i^0 + L_i^1 \|\nabla_i f(X^k)\|_{(i)\star}}{2} \left(t_i^k\right)^2 .
\end{aligned}
$$

Taking expectations, we obtain

$$
\begin{aligned}
\mathbb{E}[f(X^{k+1})] \leq \mathbb{E}[f(X^k)] + \sum_{i=1}^{p} \Bigg[& - t_i^k \mathbb{E}[\|\nabla_i f(X^k)\|_{(i)\star}] + 2t_i^k \mathbb{E}\left[\left\| M_i^k - \nabla_i f(X^k) \right\|_{(i)\star} \right] \\
& + \frac{L_i^0 + L_i^1 \mathbb{E}[\|\nabla_i f(X^k)\|_{(i)\star}]}{2} \left(t_i^k\right)^2 \Bigg].
\end{aligned}
$$

Telescoping the last inequality gives

$$
\begin{aligned}
\sum_{i=1}^{p} \sum_{k=0}^{K-1} t_i^k \mathbb{E}[\|\nabla_i f(X^k)\|_{(i)\star}] \leq \Delta^0 + \sum_{i=1}^{p} \Bigg[& 2 \sum_{k=0}^{K-1} t_i^k \mathbb{E}\left[\left\| M_i^k - \nabla_i f(X^k) \right\|_{(i)\star} \right] \\
& + \sum_{k=0}^{K-1} \frac{L_i^0}{2} \left(t_i^k\right)^2 + \sum_{k=0}^{K-1} \frac{L_i^1}{2} \mathbb{E}[\|\nabla_i f(X^k)\|_{(i)\star}] \left(t_i^k\right)^2 \Bigg],
\end{aligned} \tag{27}
$$

where $\Delta^0 := f(X^0) - \inf_{X \in \mathcal{S}} f(X)$.

Now, inspired by the analysis in Hübler et al. (2024), we introduce the following notation: $\mu_i^k := M_i^k - \nabla_i f(X^k)$, $\gamma_i^k := \nabla_i f_{\xi^k}(X^k) - \nabla_i f(X^k)$, $\alpha^k = 1 - \beta^k$, $\beta^{a:b} := \prod_{k=a}^{b} \beta^k$ and $S_i^k := \nabla_i f(X^{k-1}) - \nabla_i f(X^k)$. Then, we can rewrite the algorithm's momentum update rule as

$$
\begin{aligned}
M_i^k &= \beta^k M_i^{k-1} + (1 - \beta^k) \nabla_i f_{\xi^k}(X^k) \\
&= \beta^k \left(\mu_i^{k-1} + \nabla_i f(X^{k-1}) \right) + (1 - \beta^k) \left(\gamma_i^k + \nabla_i f(X^k) \right) \\
&= \nabla_i f\left(X^k\right) + \alpha^k \gamma_i^k + \beta^k S_i^k + \beta^k \mu_i^{k-1}.
\end{aligned}
$$

This yields

$$
\begin{aligned}
\mu_i^k &= M_i^k - \nabla_i f\left(X^k\right) \\
&= \alpha^k \gamma_i^k + \beta^k S_i^k + \beta^k \mu_i^{k-1} \\
&= \sum_{\tau=1}^{k} \beta^{(\tau+1):k} \alpha^\tau \gamma_i^\tau + \sum_{\tau=1}^{k} \beta^{\tau:k} S_i^\tau + \beta^{1:k} \mu_i^0 \\
&= \sum_{\tau=0}^{k} \beta^{(\tau+1):k} \alpha^\tau \gamma_i^\tau + \sum_{\tau=1}^{k} \beta^{\tau:k} S_i^\tau,
\end{aligned}
$$

where the last line follows from the fact that $M_i^0 = \nabla_i f_{\xi^0}(X^0)$ and $\beta^0 = 0$. Thus,

$$\begin{aligned}\mathbb{E}\left[\left\|M_i^k - \nabla_i f(X^k)\right\|_{(i)\star}\right] &= \mathbb{E}\left[\left\|\mu_i^k\right\|_{(i)\star}\right] \\ &\leq \mathbb{E}\left[\left\|\sum_{\tau=0}^{k}\beta^{(\tau+1):k}\alpha^\tau\gamma_i^\tau\right\|_{(i)\star}\right] + \sum_{\tau=1}^{k}\beta^{\tau:k}\mathbb{E}\left[\left\|S_i^\tau\right\|_{(i)\star}\right] \\ &\leq \rho_i\mathbb{E}\left[\left\|\sum_{\tau=0}^{k}\beta^{(\tau+1):k}\alpha^\tau\gamma_i^\tau\right\|_2\right] + \sum_{\tau=1}^{k}\beta^{\tau:k}\mathbb{E}\left[\left\|S_i^\tau\right\|_{(i)\star}\right] \\ &\leq \rho_i\sqrt{\sum_{\tau=0}^{k}\left(\beta^{(\tau+1):k}\alpha^\tau\right)^2\mathbb{E}\left[\left\|\gamma_i^\tau\right\|_2^2\right]} + \sum_{\tau=1}^{k}\beta^{\tau:k}\mathbb{E}\left[\left\|S_i^\tau\right\|_{(i)\star}\right],\end{aligned}$$

where in the last line we used Jensen's inequality and the fact that for all $q < l$

$$\begin{aligned}\mathbb{E}\left[(\gamma_i^l)^\top\gamma_i^q\right] &= \mathbb{E}\left[\mathbb{E}\left[(\gamma_i^l)^\top\gamma_i^q \mid X_i^l\right]\right] = \mathbb{E}\left[\mathbb{E}\left[\gamma_i^l \mid X_i^l\right]^\top\gamma_i^q\right] \\ &= \mathbb{E}\left[\left(\mathbb{E}\left[\nabla_i f_{\xi^l}(X^l) - \nabla_i f(X^l) \mid X_i^l\right]\right)^\top\gamma_i^q\right] = 0.\end{aligned}$$

Using Assumptions 1 and 2, we get

$$\mathbb{E}\left[\left\|\gamma_i^\tau\right\|_2^2\right] = \mathbb{E}\Bigg[\underbrace{\mathbb{E}\left[\left\|\gamma_i^\tau\right\|_2^2 \mid X_i^\tau\right]}_{\leq\sigma^2}\Bigg] \leq \sigma^2$$

and

$$\left\|S_i^\tau\right\|_{(i)\star} \leq \left(L_i^0 + L_i^1\|\nabla_i f(X^\tau)\|_{(i)\star}\right)\left\|X_i^{\tau+1} - X_i^\tau\right\|_{(i)} \leq \left(L_i^0 + L_i^1\|\nabla_i f(X^\tau)\|_{(i)\star}\right)t_i^\tau.$$

Therefore,

$$\begin{aligned}\mathbb{E}\left[\left\|M_i^k - \nabla_i f(X^k)\right\|_{(i)\star}\right] \quad\leq\quad & \sigma\rho_i\sqrt{\sum_{\tau=0}^{k}\left(\beta^{(\tau+1):k}\alpha^\tau\right)^2} + L_i^0\sum_{\tau=1}^{k}\beta^{\tau:k}t_i^\tau \\ & + L_i^1\sum_{\tau=1}^{k}\beta^{\tau:k}t_i^\tau\mathbb{E}\left[\|\nabla_i f(X^\tau)\|_{(i)\star}\right].\end{aligned}$$

Combining the last inequality with (27) gives

$$\begin{aligned}&\sum_{i=1}^{p}\sum_{k=0}^{K-1}t_i^k\mathbb{E}[\|\nabla_i f(X^k)\|_{(i)\star}] \\ &\quad\leq \Delta^0 + \sum_{i=1}^{p}\Bigg[\underbrace{2\sigma\rho_i\sum_{k=0}^{K-1}t_i^k\sqrt{\sum_{\tau=0}^{k}\left(\beta^{(\tau+1):k}\alpha^\tau\right)^2}}_{=:I_1} + \underbrace{2L_i^0\sum_{k=0}^{K-1}t_i^k\sum_{\tau=1}^{k}\beta^{\tau:k}t_i^\tau}_{=:I_2} \\ &\qquad + \underbrace{2L_i^1\sum_{k=0}^{K-1}t_i^k\sum_{\tau=1}^{k}\beta^{\tau:k}t_i^\tau\mathbb{E}\left[\|\nabla_i f(X^\tau)\|_{(i)\star}\right]}_{=:I_3} \\ &\qquad + \underbrace{\frac{L_i^0}{2}\sum_{k=0}^{K-1}\left(t_i^k\right)^2}_{=:I_4} + \frac{L_i^1}{2}\sum_{k=0}^{K-1}\left(t_i^k\right)^2\mathbb{E}\left[\|\nabla_i f(X^k)\|_{(i)\star}\right]\Bigg].\end{aligned} \tag{28}$$

Let us now upper-bound each term I_i, $i = 1, 2, 3, 4$.

I_1: using Lemma 5, we obtain

$$I_1 \leq \sigma\rho_i t_i \left(7 + 2\sqrt{2e^2}\log(K)\right).$$

I_2: using Lemma 5, we obtain

$$I_2 \leq 14 L_i^0 t_i^2 \left(3 + \log(K)\right).$$

I_3: rearranging the sums and using Lemma 4 with $a = \tau + 1$, $b = K$, $p = 3/4$ and $q = 1/2$, we have

$$\begin{aligned}
I_3 &= 2L_i^1 \sum_{k=0}^{K-1} t_i^k \sum_{\tau=1}^{k} \beta^{\tau:k} t_i^\tau \mathbb{E}\left[\|\nabla_i f(X^\tau)\|_{(i)\star}\right] \\
&= 2L_i^1 \sum_{\tau=1}^{K-1} t_i^\tau \left(\sum_{k=\tau}^{K-1} t_i^k \beta^{\tau:k}\right) \mathbb{E}\left[\|\nabla_i f(X^\tau)\|_{(i)\star}\right] \\
&= 2L_i^1 \sum_{\tau=1}^{K-1} t_i^\tau t_i \left(\sum_{k=\tau}^{K-1} (k+1)^{-3/4} \beta^{\tau:k}\right) \mathbb{E}\left[\|\nabla_i f(X^\tau)\|_{(i)\star}\right] \\
&\leq 2L_i^1 \sum_{\tau=1}^{K-1} t_i^\tau t_i \tau^{-1/4} \underbrace{e^{2\left((\tau+1)^{1/2} - \tau^{1/2}\right)}}_{\leq e^{2(\sqrt{2}-1)} \text{ for } \tau \geq 1} \mathbb{E}\left[\|\nabla_i f(X^\tau)\|_{(i)\star}\right] \\
&\leq 2e^{2(\sqrt{2}-1)} L_i^1 \sum_{\tau=1}^{K-1} t_i^\tau t_i \tau^{-1/4} \mathbb{E}\left[\|\nabla_i f(X^\tau)\|_{(i)\star}\right] \\
&\leq 2e^{2(\sqrt{2}-1)} L_i^1 \sum_{k=0}^{K-1} t_i^k t_i \mathbb{E}\left[\|\nabla_i f(X^k)\|_{(i)\star}\right].
\end{aligned}$$

I_4:

$$\begin{aligned}
I_4 &= \frac{L_i^0}{2} \sum_{k=0}^{K-1} \left(t_i^k\right)^2 \leq \frac{L_i^0}{2} \sum_{k=0}^{\infty} \left(t_i^k\right)^2 = \frac{L_i^0}{2} t_i^2 \sum_{k=0}^{\infty} (1+k)^{-3/2} \\
&\leq \frac{L_i^0}{2} t_i^2 \left(1 + \int_1^\infty \frac{1}{z^{3/2}}\, dz\right) = \frac{3L_i^0}{2} t_i^2.
\end{aligned}$$

Combining the upper-bounds for I_i, $i = 1, 2, 3, 4$ with (28) gives

$$\begin{aligned}
\sum_{i=1}^{p} \sum_{k=0}^{K-1} t_i^k \mathbb{E}[\|\nabla_i f(X^k)\|_{(i)\star}] \leq \Delta^0 + \sum_{i=1}^{p} \Bigg[& \sigma\rho_i t_i \left(7 + 2\sqrt{2e^2}\log(K)\right) + 14 L_i^0 t_i^2 \left(3 + \log(K)\right) \\
& + 2e^{2(\sqrt{2}-1)} L_i^1 \sum_{k=0}^{K-1} t_i^k t_i \mathbb{E}\left[\|\nabla_i f(X^k)\|_{(i)\star}\right] \\
& + \frac{3L_i^0}{2} t_i^2 + \frac{L_i^1}{2} \sum_{k=0}^{K-1} \left(t_i^k\right)^2 \mathbb{E}[\|\nabla_i f(X^k)\|_{(i)\star}] \Bigg].
\end{aligned}$$

Using the fact that $t_i^k = t_i(1+k)^{-3/4} \leq t_i$, and denoting $C := 2e^{2(\sqrt{2}-1)} + \frac{1}{2} \leq 5.1$, we get

$$\begin{aligned}
\sum_{i=1}^{p} \sum_{k=0}^{K-1} t_i^k \mathbb{E}[\|\nabla_i f(X^k)\|_{(i)\star}] \leq \Delta^0 + \sum_{i=1}^{p} \Bigg[& \sigma\rho_i t_i \left(7 + 2\sqrt{2e^2}\log(K)\right) + 14 L_i^0 t_i^2 \left(\frac{87}{28} + \log(K)\right) \\
& + C L_i^1 t_i \sum_{k=0}^{K-1} t_i^k \mathbb{E}\left[\|\nabla_i f(X^k)\|_{(i)\star}\right] \Bigg].
\end{aligned}$$

Now, let us consider two options: (1) $L_i^1 = 0$ for all $i \in \{1, \ldots, p\}$ and (2) $L_i^1 \neq 0$, for all $i \in \{1, \ldots, p\}$.

Case 1: $L_i^1 = 0$**,** $i = 1, \ldots, p$**.** In this case,

$$\sum_{i=1}^{p} \sum_{k=0}^{K-1} t_i^k \mathbb{E}[\|\nabla_i f(X^k)\|_{(i)\star}] \leq \Delta^0 + \sum_{i=1}^{p} \left[\sigma \rho_i t_i \left(7 + 2\sqrt{2e^2}\log(K)\right) + 14 L_i^0 t_i^2 \left(\frac{87}{28} + \log(K)\right) \right],$$

and therefore,

$$\begin{aligned}
&\min_{k=0,\ldots,K-1} \sum_{i=1}^{p} t_i \mathbb{E}[\|\nabla_i f(X^k)\|_{(i)\star}] \\
&\quad \leq \frac{1}{K} \sum_{k=0}^{K-1} \sum_{i=1}^{p} t_i \mathbb{E}[\|\nabla_i f(X^k)\|_{(i)\star}] \\
&\quad \leq \frac{1}{K^{1/4}} \sum_{k=0}^{K-1} \sum_{i=1}^{p} t_i (1+k)^{-3/4} \mathbb{E}[\|\nabla_i f(X^k)\|_{(i)\star}] \\
&\quad = \frac{1}{K^{1/4}} \sum_{k=0}^{K-1} \sum_{i=1}^{p} t_i^k \mathbb{E}[\|\nabla_i f(X^k)\|_{(i)\star}] \\
&\quad \leq \frac{\Delta^0}{K^{1/4}} + \frac{1}{K^{1/4}} \sum_{i=1}^{p} \left[\sigma \rho_i t_i \left(7 + 2\sqrt{2e^2}\log(K)\right) + L_i^0 t_i^2 \left(\frac{87}{2} + 14\log(K)\right) \right].
\end{aligned}$$

Case 2: $L_i^1 \neq 0$**,** $i = 1, \ldots, p$**.** Let us choose $t_i = \frac{1}{12 L_i^1}$. Then

$$\sum_{i=1}^{p} \sum_{k=0}^{K-1} t_i^k \mathbb{E}[\|\nabla_i f(X^k)\|_{(i)\star}] \leq 2\Delta^0 + \sum_{i=1}^{p} \left[2\sigma \rho_i t_i \left(7 + 2\sqrt{2e^2}\log(K)\right) + L_i^0 t_i^2 \left(87 + 28\log(K)\right) \right],$$

and hence

$$\begin{aligned}
&\min_{k=0,\ldots,K-1} \sum_{i=1}^{p} \frac{1}{12 L_i^1} \mathbb{E}[\|\nabla_i f(X^k)\|_{(i)\star}] \\
&\quad \leq \frac{1}{K} \sum_{k=0}^{K-1} \sum_{i=1}^{p} t_i \mathbb{E}[\|\nabla_i f(X^k)\|_{(i)\star}] \\
&\quad \leq \frac{1}{K^{1/4}} \sum_{k=0}^{K-1} \sum_{i=1}^{p} t_i (1+k)^{-3/4} \mathbb{E}[\|\nabla_i f(X^k)\|_{(i)\star}] \\
&\quad = \frac{1}{K^{1/4}} \sum_{i=1}^{p} \sum_{k=0}^{K-1} t_i^k \mathbb{E}[\|\nabla_i f(X^k)\|_{(i)\star}] \\
&\quad \leq \frac{2\Delta^0}{K^{1/4}} + \frac{1}{K^{1/4}} \sum_{i=1}^{p} \left[\frac{\sigma \rho_i}{6 L_i^1} \left(7 + 2\sqrt{2e^2}\log(K)\right) + \frac{L_i^0}{144 (L_i^1)^2} \left(87 + 28\log(K)\right) \right].
\end{aligned}$$

□

F Additional experimental results and details

F.1 Experimental details

All experiments for the `NanoGPT` model are conducted using PyTorch[7] with Distributed Data Parallel (DDP)[8] across 4 NVIDIA A100 GPUs (40GB each). For the `CNN` experiments, training is performed on a single NVIDIA A100 GPU (40GB). The training and evaluation pipelines are implemented using open-source codebases (Jordan, 2024; Jordan et al., 2024a; Pethick et al., 2025a), with all modifications clearly documented and properly referenced where applicable.

For LMO-based methods, we compute inexact LMOs using the Newton–Schulz iteration when an analytical solution is unavailable (e.g., for SVD-type updates), following the approach proposed by Jordan et al. (2024b). This method provides a computationally efficient approximation of the required orthogonalization while preserving the convergence behavior of the overall algorithm.

F.2 Fitting L_i^0 and L_i^1

To minimize the Euclidean error between the true value $\hat{L}_i[k]$ and its approximation $\hat{L}_i^{\text{approx}}[k]$, while penalizing underestimation, we incorporate a hinge-like penalty term. Specifically, we fit L_i^0 and L_i^1 by minimizing the loss function

$$\mathcal{L}_i\left(L_i^0, L_i^1\right) := \sum_{k=0}^{K-1} \left(\hat{L}_i[k] - \hat{L}_i^{\text{approx}}[k]\right)^2 + \lambda \sum_{k=0}^{K-1} \max\left(0, \hat{L}_i[k] - \hat{L}_i^{\text{approx}}[k]\right)^2. \tag{29}$$

The first term of $\mathcal{L}_i$ captures the standard Euclidean (squared) error, while the second term introduces an additional penalty proportional to the amount of underestimation (i.e., when $\hat{L}_i[k] > \hat{L}_i^{\text{approx}}[k]$). The hyperparameter $\lambda \geq 0$ controls the strength of this penalty.

F.3 Training NanoGPT on FineWeb.

In this section, we present additional results and experimental details for the experiment described in the main text, which involves training a `NanoGPT` model on the `FineWeb` dataset using the unScion optimizer.

F.3.1 Empirical validation of Assumption 1

We begin by presenting additional results for the experiment described in Section 5.1, aimed at empirically validating Assumption 1. We plot the estimated *trajectory smoothness*

$$\hat{L}_i[k] := \frac{\|\nabla_i f_{\xi^{k+1}}(X^{k+1}) - \nabla_i f_{\xi^k}(X^k)\|_{(i)\star}}{\|X_i^{k+1} - X_i^k\|_{(i)}}$$

and its approximation

$$\hat{L}_i^{\text{approx}}[k] := L_i^0 + L_i^1 \|\nabla_i f_{\xi^{k+1}}(X^{k+1})\|_{(i)\star}$$

as functions of the iteration index k, where $L_i^0, L_i^1 \geq 0$ are fitted using the procedure described in Appendix F.2.

Figures 5, 6, and 7 show results for parameter groups from the embedding layer and from the 4th and 8th transformer blocks. Similar patterns are observed across all layers. In each case, we see a strong agreement between $\hat{L}_i[k]$ and $\hat{L}_i^{\text{approx}}[k]$, suggesting that Assumption 1 holds approximately along the optimization trajectory.

[7] PyTorch Documentation. Available at: https://pytorch.org/docs/stable/index.html

[8] Distributed Data Parallel (DDP) in PyTorch. Available at: https://pytorch.org/docs/stable/notes/ddp.html

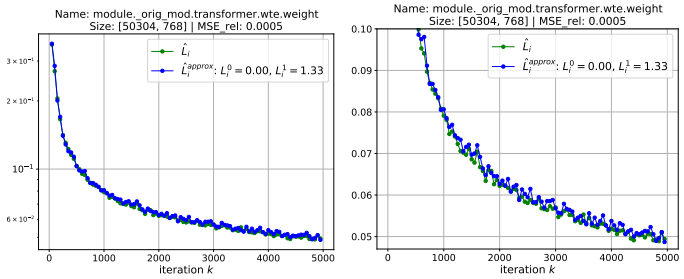

Figure 5: Validation of layer-wise (L^0, L^1)-smoothness for the group of parameters from the embedding layer of `NanoGPT-124M` along unScion training trajectories. The group norm is $\|\cdot\|_{(p)} = n_p\|\cdot\|_{1\to\infty}$, with fitted values $L_p^0 \approx 0$, $L_p^1 \approx 1.3$. The same plot is shown twice with different y-axis limits.

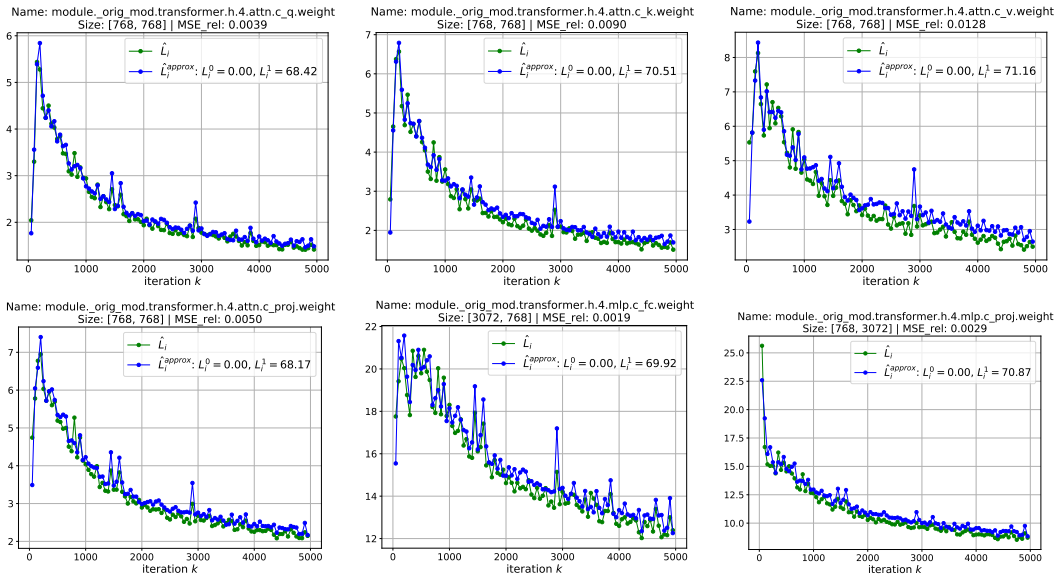

Figure 6: Validation of layer-wise (L^0, L^1)-smoothness for the group of parameters from the 4th transformer block of `NanoGPT-124M` along unScion training trajectories. The group norms are $\|\cdot\|_{(i)} = \sqrt{n_i/m_i}\|\cdot\|_{2\to 2}$, with fitted values $L_i^0 \approx 0$, $L_i^1 \approx 70$.

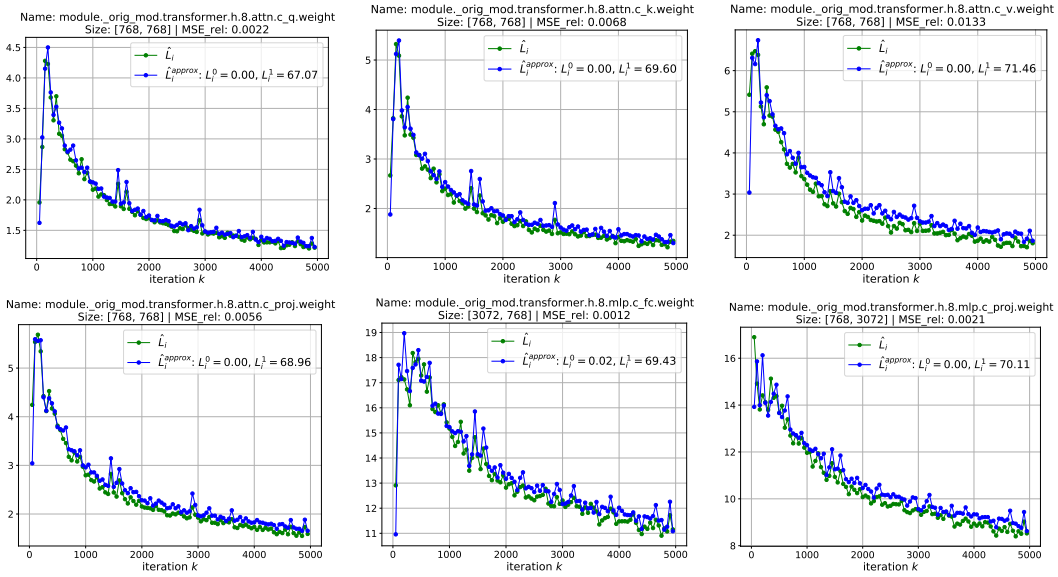

Figure 7: Validation of layer-wise (L^0, L^1)-smoothness for the group of parameters from the 8th transformer block of `NanoGPT-124M` along unScion training trajectories. The group norms are $\|\cdot\|_{(i)} = \sqrt{n_i/m_i}\|\cdot\|_{2\to 2}$, with fitted values $L_i^0 \approx 0$, $L_i^1 \approx 70$.

F.3.2 Generalized smoothness under Euclidean vs. specialized norms

In this experiment, we compare how well the layer-wise (L^0, L^1)-smoothness assumption is satisfied under the standard Euclidean norms $\|\cdot\|_2$ for each parameter block, as opposed to the specialized norms described in (14). We adopt the same training setup as in Section 5.1, plotting the estimated trajectory smoothness $\hat{L}_i$ and its approximation $\hat{L}_i^{\text{approx}}$ along the training trajectories across several parameter groups. Unlike previous sections, here we do not penalize instances where $\hat{L}_i > \hat{L}_i^{\text{approx}}$ in order to find the best approximation (i.e., $\lambda = 0$ in (29)). Additionally, when using the standard Euclidean norm $\|\cdot\|_2$ for approximation, we exclude the first point, as it could distort the result.

We evaluate the quality of each approximation using the relative mean squared error ($\text{MSE}_i^{\text{rel}}$, denoted MSE_rel in the figures), defined as

$$\text{MSE}_i^{\text{rel}} := \frac{1}{K}\sum_{i=1}^{K}\left(\frac{\hat{L}_i[k] - \hat{L}_i^{\text{approx}}[k]}{\hat{L}_i[k]}\right)^2,$$

where a lower value indicates a better fit.

As shown in Figures 8 and 9, both visually and in terms of $\text{MSE}_i^{\text{rel}}$, using specialized norms for each group of parameters provides a better approximation than the standard Euclidean norm $\|\cdot\|_2$. Notably, the relative mean squared error $\text{MSE}_i^{\text{rel}}$ is consistently an order of magnitude lower under specialized norms.

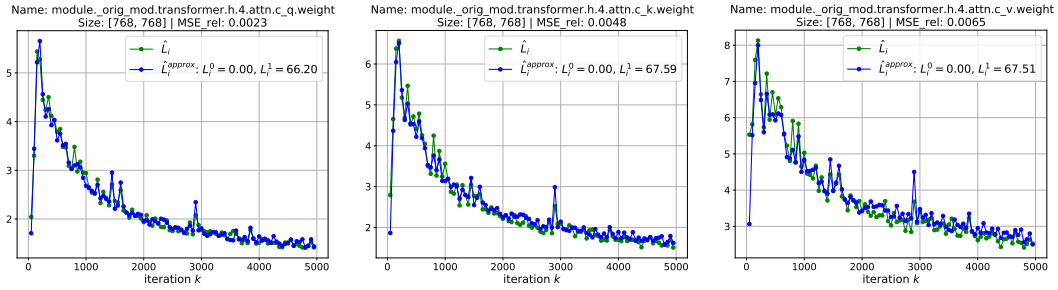

(a) $\mathrm{MSE}_i^{\mathrm{rel}} = 0.0023$ (b) $\mathrm{MSE}_i^{\mathrm{rel}} = 0.0048$ (c) $\mathrm{MSE}_i^{\mathrm{rel}} = 0.0065$

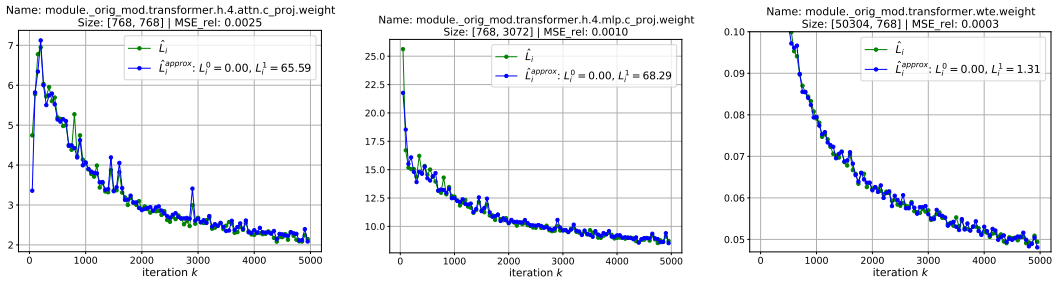

(d) $\mathrm{MSE}_i^{\mathrm{rel}} = 0.0025$ (e) $\mathrm{MSE}_i^{\mathrm{rel}} = 0.001$ (f) $\mathrm{MSE}_i^{\mathrm{rel}} = 0.0003$

Figure 8: Validation of layer-wise (L^0, L^1)-smoothness for different groups of parameters in `NanoGPT-124M` along training trajectories of unScion using the specialized norm choices defined in (14).

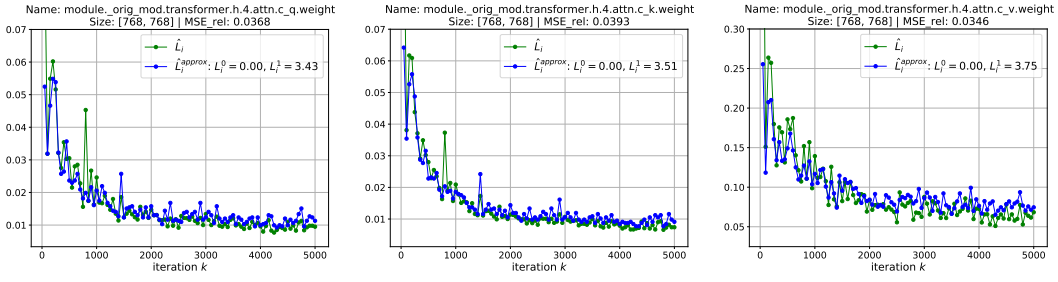

(a) $\mathrm{MSE}_i^{\mathrm{rel}} = 0.0368$ (b) $\mathrm{MSE}_i^{\mathrm{rel}} = 0.0393$ (c) $\mathrm{MSE}_i^{\mathrm{rel}} = 0.0346$

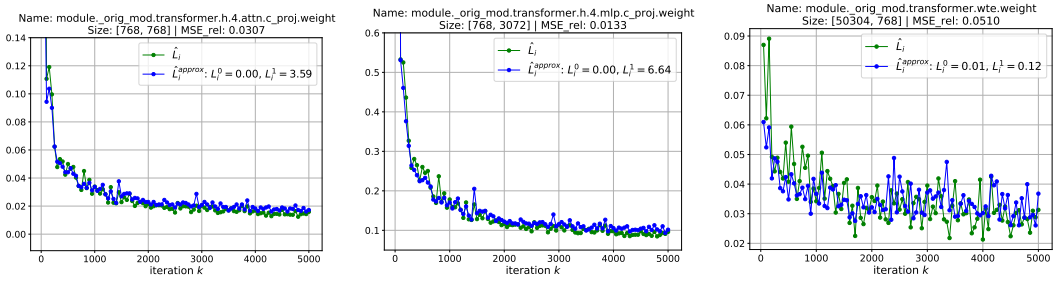

(d) $\mathrm{MSE}_i^{\mathrm{rel}} = 0.0307$ (e) $\mathrm{MSE}_i^{\mathrm{rel}} = 0.0133$ (f) $\mathrm{MSE}_i^{\mathrm{rel}} = 0.051$

Figure 9: Validation of layer-wise (L^0, L^1)-smoothness for different groups of parameters in `NanoGPT-124M` along training trajectories of unScion using the standard Euclidean norm $\|\cdot\|_2$.

F.3.3 Learning rate transfer from AdamW

We now aim to verify layer-wise (L^0, L^1)-smoothness following the approach used in Section 5.1, but employing the AdamW optimizer. We use hyperparameters specified in Pethick et al. (2025b, Table 7). In Figure 10, we present the results for the estimated trajectory smoothness $\hat{L}_i$ and its approximation $\hat{L}_i^{\text{approx}}$ across several parameter groups along the training trajectories. Notably, for the group of parameters from the embedding layer X_p (the last plot in Figure 10), the fitted value of L_p^1 is approximately 20–30 times smaller than in other groups. Since in all plots we observe that

$L_i^0 \ll L_i^1 \|\nabla_i f_{\xi^k}(X^k)\|_{(i)\star}$, Theorem 1 implies that $t_i^k \approx 1/L_i^k$. Thus, t_p^k should be 20–30 times larger than t_i^k for $i = 1, \ldots, p-1$, which is consistent with the tuned parameters from Pethick et al. (2025b, Table 7).

This insight provides an efficient and principled method for initializing learning rates in Scion. Smoothness statistics collected during standard AdamW training (which is commonly used for training LLMs) can serve as a strong prior, allowing practitioners to directly incorporate structure-aware choices, such as larger stepsizes for embedding layers, into their tuning process. Importantly, computing these statistics is computationally inexpensive, introducing minimal additional cost.

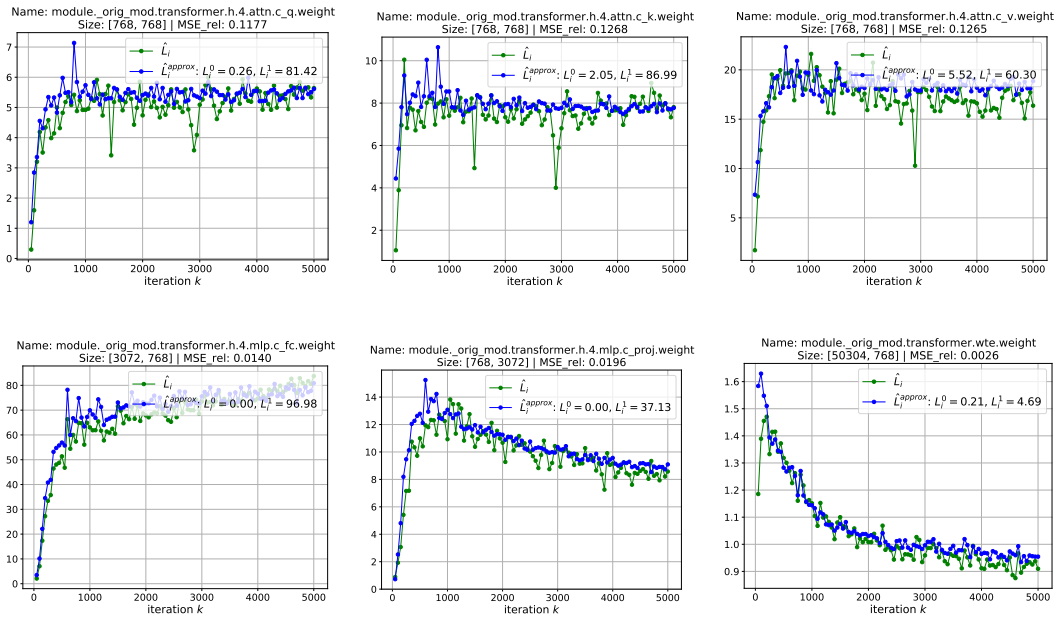

Figure 10: Validation of layer-wise (L^0, L^1)-smoothness for different groups of parameters in `NanoGPT-124M` along AdamW training trajectories.

F.4 Training CNN on CIFAR-10

In this section, we provide additional results for the experiments described in Section 5.2, where a `CNN` model is trained on the `CIFAR-10` dataset using the unScion optimizer.

Full-batch (deterministic) gradients. We begin with presenting additional results in the deterministic setting. Figure 11 shows the estimated trajectory smoothness

$$\hat{L}_i[k] := \frac{\|\nabla_i f(X^{k+1}) - \nabla_i f(X^k)\|_{(i)\star}}{\|X_i^{k+1} - X_i^k\|_{(i)}}$$

and its approximation

$$\hat{L}_i^{\text{approx}}[k] := L_i^1 \|\nabla_i f(X^{k+1})\|_{(i)\star}$$

(where we set $L_i^0 = 0$) for a broader selection of parameter groups than shown in the main text. The results further support the validity of Assumption 1 with $L_i^0 = 0$.

Stochastic gradients. Here, we report results for analogous experiments in the stochastic setting, using noisy gradients $\nabla_i f_{\xi^k}$. We use momentum as in Pethick et al. (2025b, Table 10), but do not apply a linear decay schedule. In Figure 12, we plot

$$\hat{L}_i[k] = \frac{\|\nabla_i f_{\xi^{k+1}}(X^{k+1}) - \nabla_i f_{\xi^k}(X^k)\|_{(i)\star}}{\|X_i^{k+1} - X_i^k\|_{(i)}}, \qquad \hat{L}_i^{\text{approx}}[k] = L_i^1 \|\nabla_i f_{\xi^{k+1}}(X^{k+1})\|_\star,$$

again setting $L_i^0 = 0$. Despite the added variance, we still observe that the stochastic trajectory roughly adheres to Assumption 1.

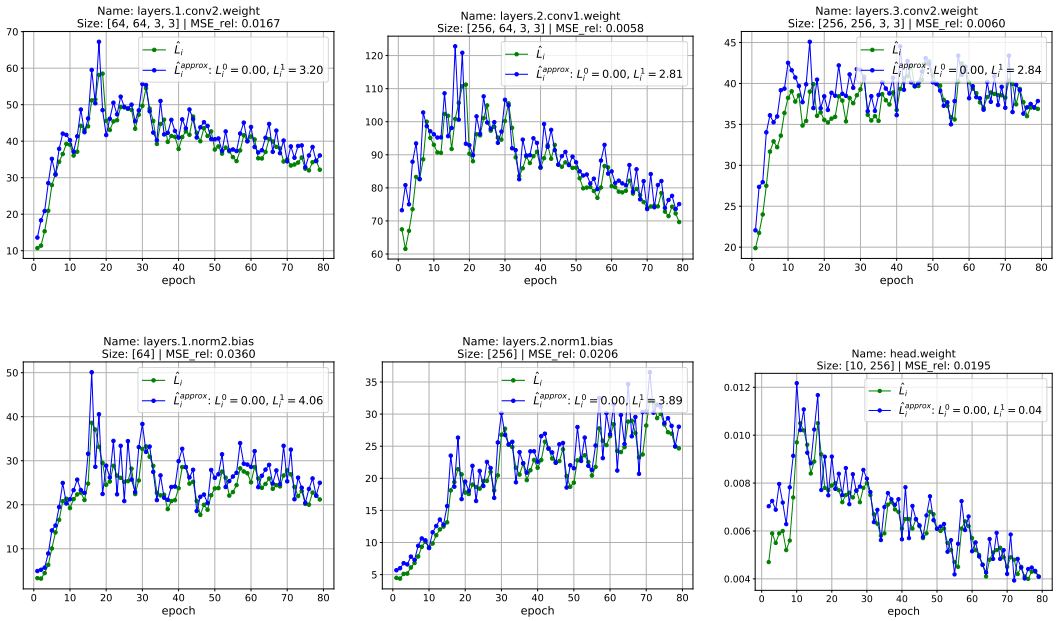

Figure 11: Validation of layer-wise (L^0, L^1)-smoothness for different groups of parameters of a CNN model along the training trajectories of unScion with **full-batch gradients**. The norms used for each group are as follows: $\|\cdot\|_{(i)} = \sqrt{1/C_i^{out}}\|\cdot\|_2$ for biases, $\|\cdot\|_{(i)} = k^2\sqrt{C_i^{in}/C_i^{out}}\|\cdot\|_{2\to 2}$ for conv, and $\|\cdot\|_{(p)} = n_p\|\cdot\|_{1\to\infty}$ for the last group X_p, associated with classification head weights.

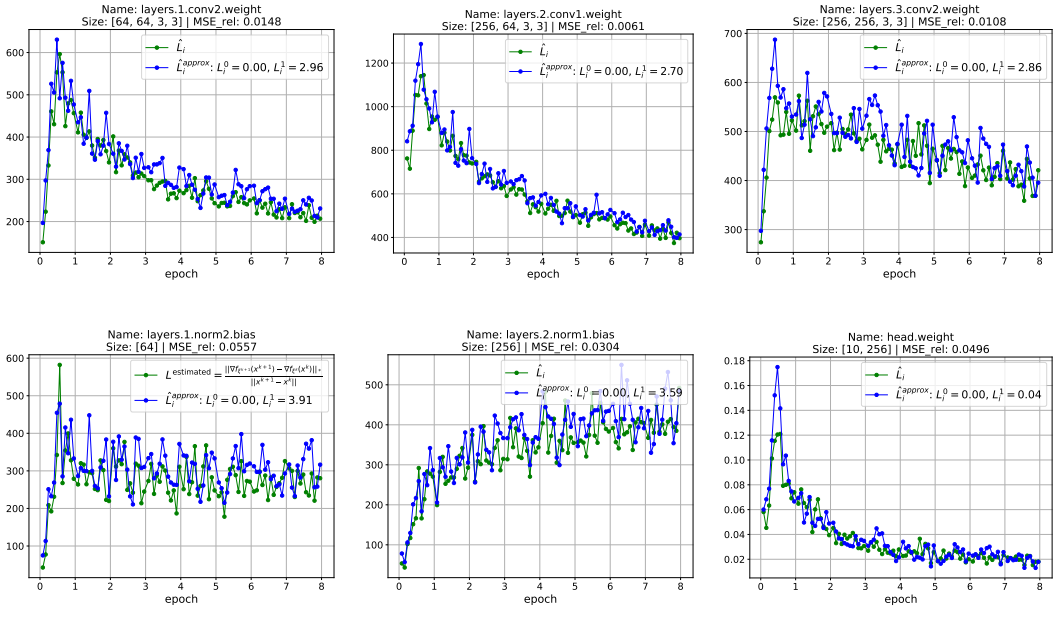

Figure 12: Validation of layer-wise (L^0, L^1)-smoothness for different groups of parameters of a CNN model along the training trajectories of unScion with **stochastic gradients**. The norms used for each group are as follows: $\|\cdot\|_{(i)} = \sqrt{1/C_i^{out}}\|\cdot\|_2$ for biases, $\|\cdot\|_{(i)} = k^2\sqrt{C_i^{in}/C_i^{out}}\|\cdot\|_{2\to 2}$ for conv, and $\|\cdot\|_{(p)} = n_p\|\cdot\|_{1\to\infty}$ for the last group X_p, associated with classification head weights.

G Additional Empirical Results

G.1 Layer-wise smoothness across all layers and varied model scales

Aggregate layer-wise trajectory smoothness across all blocks/layers. The cross-layer heterogeneity and the empirical trend $L_i^0 \approx 0$ persist from 124M to 774M parameters.

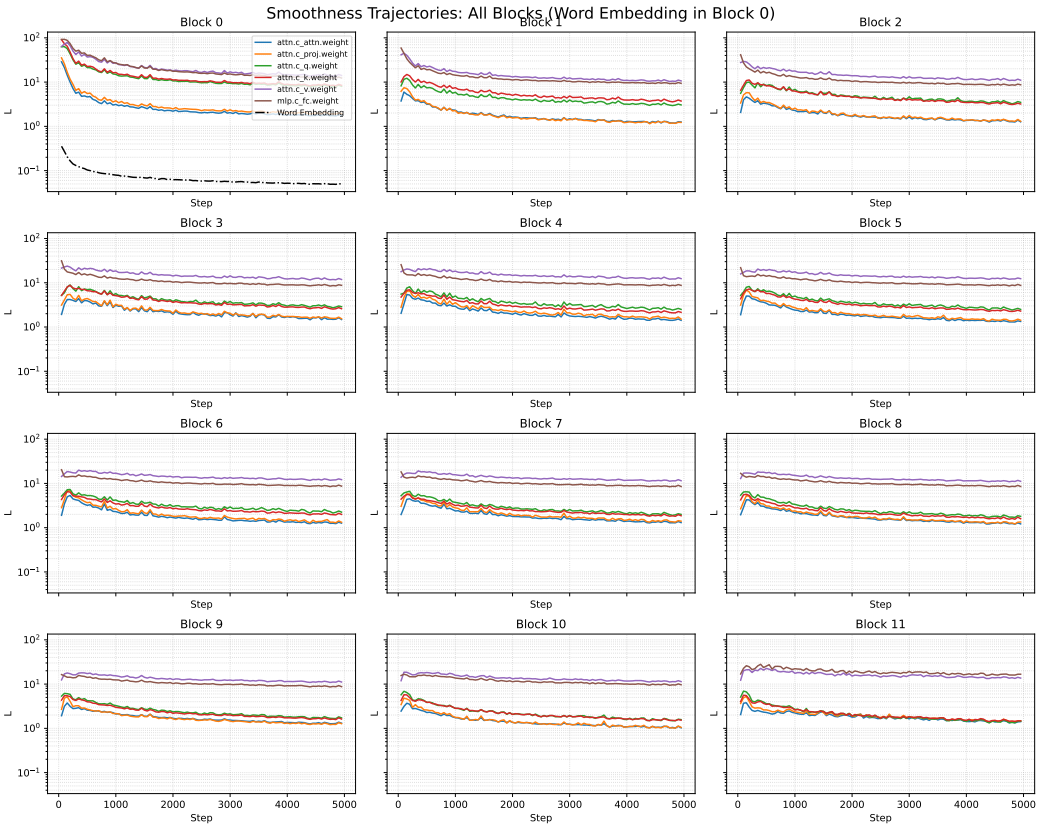

Figure 13: `NanoGPT-124M`

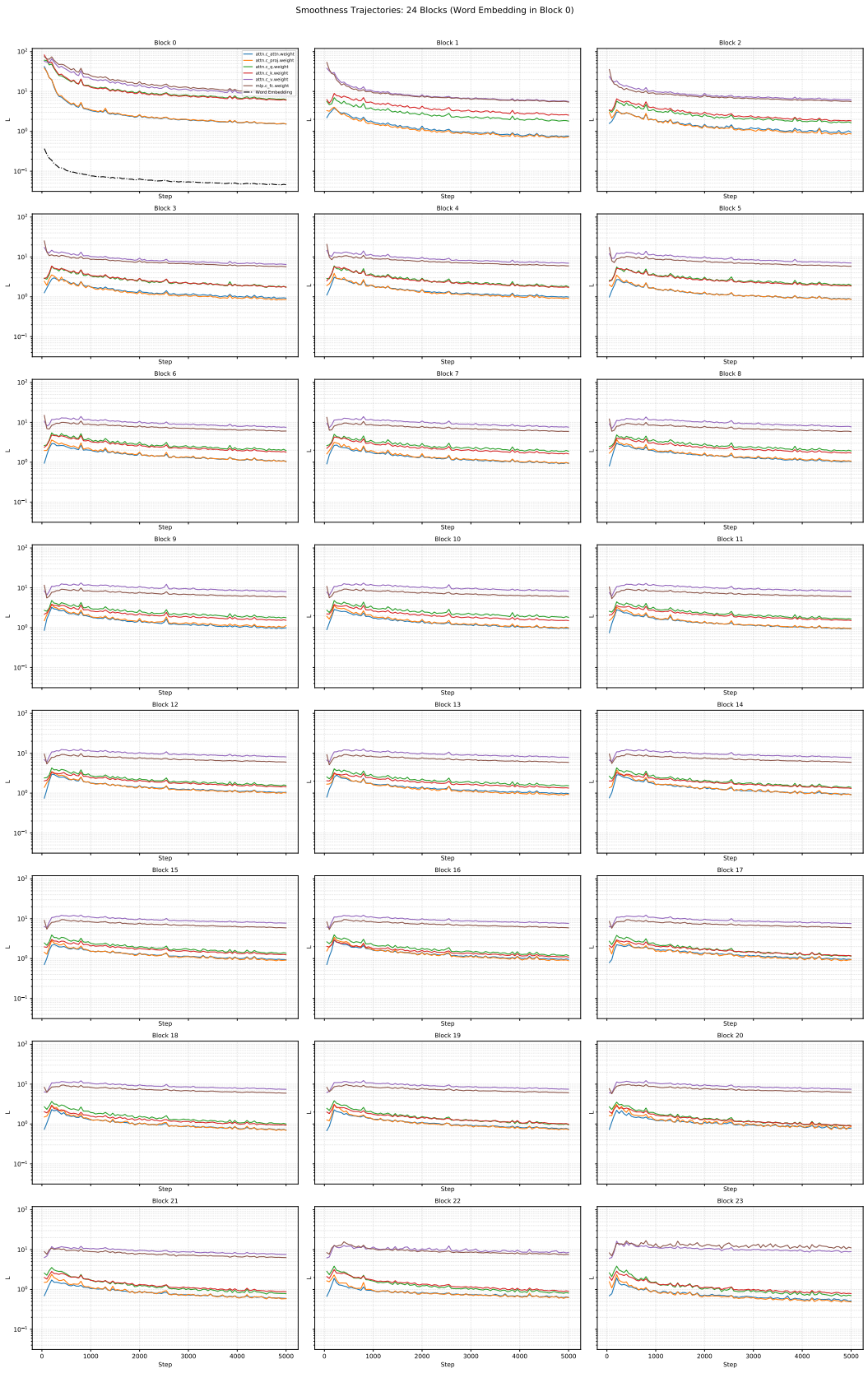

Figure 14: `GPT-2 Medium` (∼355M)

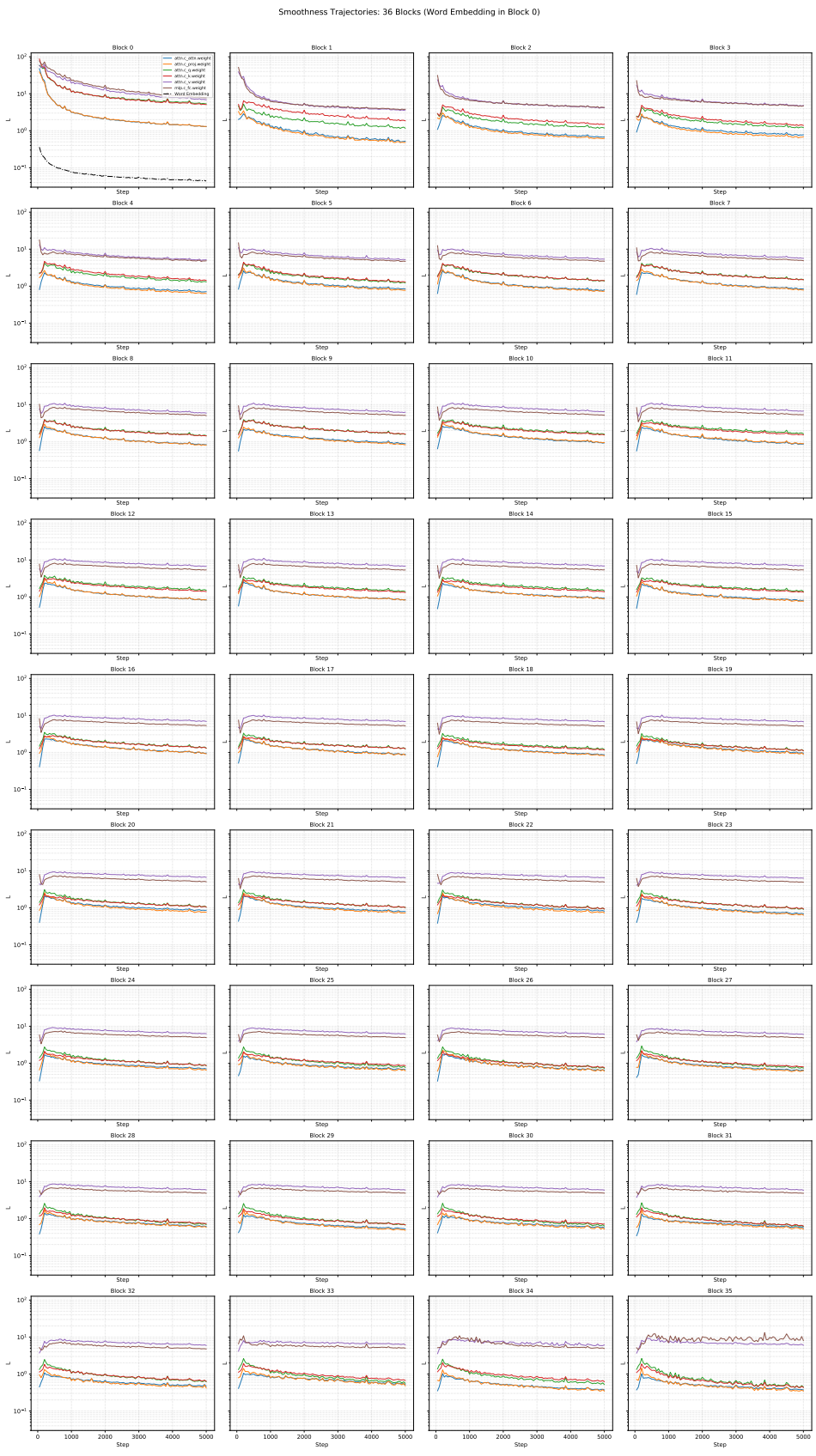

Figure 15: `GPT-2 Large` (∼774M)

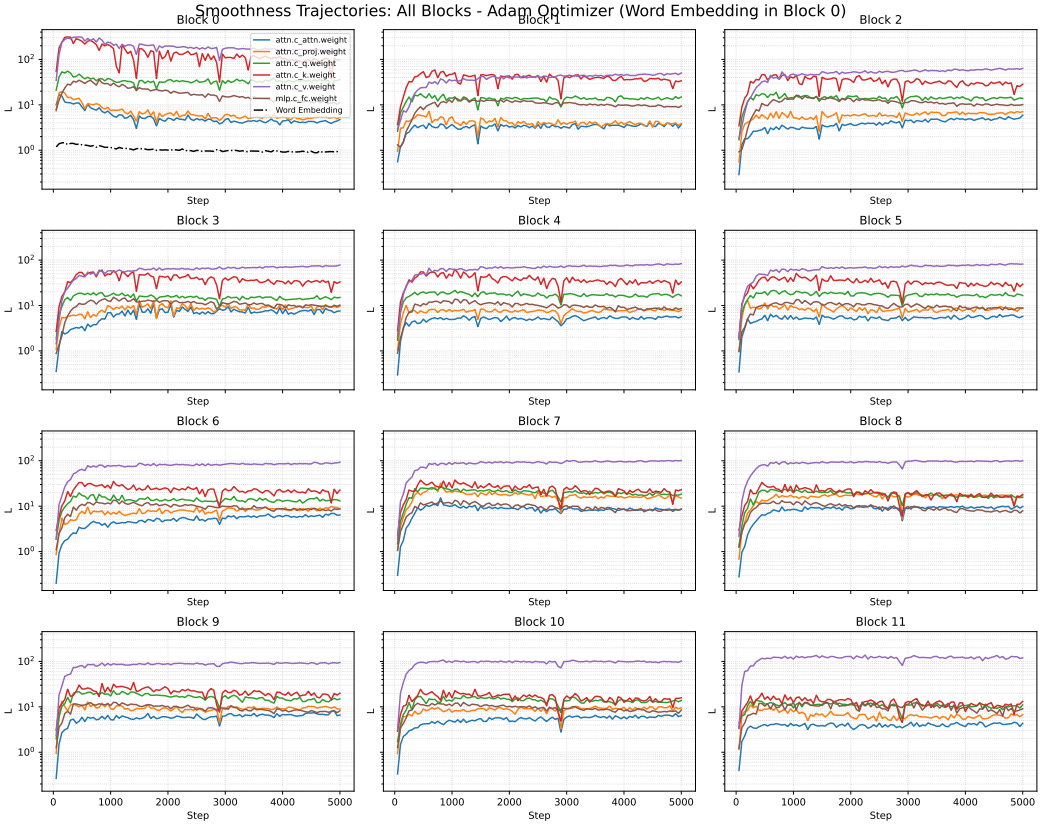

Figure 16: `NanoGPT-124M` trained with AdamW. The same cross-layer heterogeneity pattern persists, indicating that layer-wise (L_i^0, L_i^1)-smoothness is not specific to unScion.

G.2 BEST VS. WORST FITS AND AGGREGATE FIT QUALITY

Figure 17 illustrates best and worst per-layer fits of Assumption 1 (measured $L_i[k]$ vs. $L_i^{\text{approx}}[k]$) along `NanoGPT-124M` training. We observe tight fits for many layers (e.g., embeddings and several attention V matrices), while a few layers show looser—yet still bounded—fits. The model error is more than $10\times$ smaller than for constant-L_i fits on most layers, and in some cases smaller by orders of magnitude.

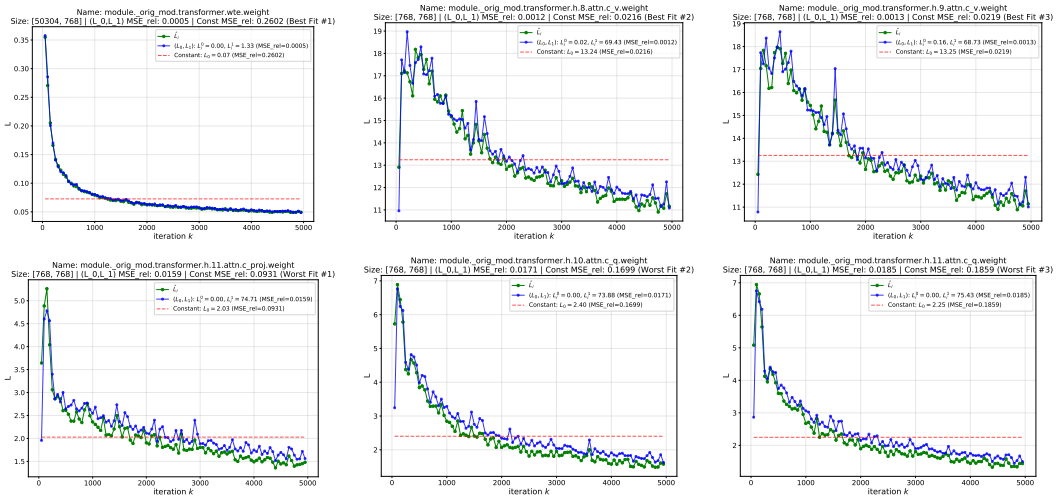

Figure 17: Illustrative *best* (top row) and *worst* (bottom row) per-layer fits of Assumption 1 (measured $L_i[k]$ vs. $L_i^{\text{approx}}[k]$) along `NanoGPT-124M` training.

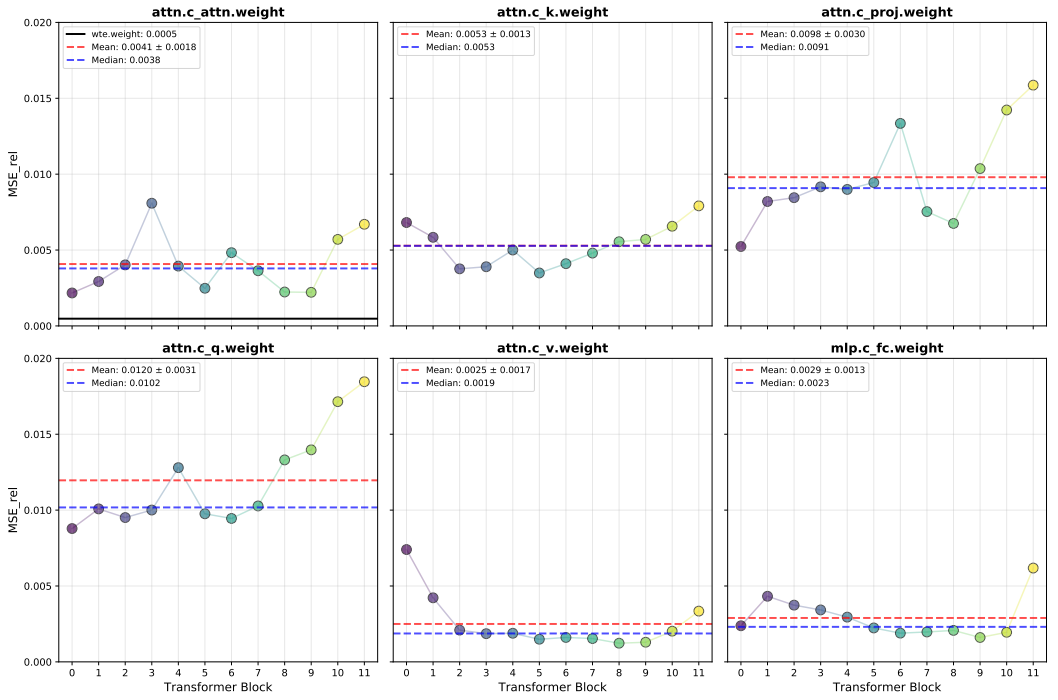

Figure 18: Relative fit error MSE_{rel} of the layer-wise (L_i^0, L_i^1) model across transformer blocks for each matrix type in `NanoGPT-124M`. Dashed lines show mean and median over blocks (embedding matrix: $\text{MSE}_{\text{rel}} = 0.0005$).